PHYSICAL REVIEW D **72**, 114018 (2005)

Nonlinear $k_\perp$ factorization for gluon-gluon dijets produced off nuclear targets

N. N. Nikolaev,[1,2,*] W. Schäfer,[1,†] and B. G. Zakharov[2,1,‡]
[1] *Institut für Kernphysik, Forschungszentrum Jülich, D-52425 Jülich, Germany*
[2] *L. D. Landau Institute for Theoretical Physics, Moscow 117940, Russia*
(Received 31 August 2005; published 23 December 2005)

The origin of the breaking of conventional linear $k_\perp$ factorization for hard processes in a nuclear environment is by now well established. The realization of the nonlinear nuclear $k_\perp$ factorization which emerges instead was found to change from one jet observable to another. A basic ingredient of the master formula for the dijet spectrum is the S matrix for color-singlet multiparton states, and here we report on an important technical progress, the evaluation of the four-gluon color-dipole cross section operator. It describes the coupled seven-channel non-Abelian intranuclear evolution of the four-gluon color-singlet states. An exact diagonalization of this seven-channel problem is possible for large number of colors N_c and allows a formulation of nonlinear $k_\perp$ factorization for production of gluon-gluon dijets. The momentum spectra for dijets in all possible color representations are reported in the form of explicit quadratures in terms of the collective nuclear unintegrated glue. Our results fully corroborate the concept of universality classes.

DOI: 10.1103/PhysRevD.72.114018 PACS numbers: 13.87.−a, 11.80.La, 12.38.Bx, 13.85.−t

I. INTRODUCTION

The key point behind conventional perturbative quantum chromo dynamics (pQCD) factorization theorems is that parton densities are low and a single parton from the beam and a single parton from the target participate in a hard reaction. As a result, hard cross sections are linear functionals (convolutions) of the appropriate parton densities in the projectile and target [1]. For instance, once the unintegrated gluon density of the target proton is determined from the deep inelastic scattering (DIS) structure function, it would allow a consistent description of all other small x, i.e., high-energy, processes of hard production off free nucleons. In contrast to that, in hard production off nuclei the contributions of multigluon exchanges with the nucleus are enhanced by a large size of the target. The principal consequence is a dramatic breaking of the conventional linear $k_\perp$ factorization for hard processes in a nuclear environment which, according to the recent extensive studies [2–6], must be replaced by a nonlinear $k_\perp$ factorization. Namely, one can take diffractive dijet production [7,8] as a reference process for the definition of the collective nuclear unintegrated gluon density. Then, it turns out that the so-defined nuclear glue furnishes the familiar linear $k_\perp$ factorization description of the nuclear structure function $F_{2A}(x, Q^2)$ and of the forward single-quark spectrum in DIS (although the linear $k_\perp$ factorization property of both observables is rather an exception due to the Abelian feature of the photon). Furthermore, the dijet spectra in DIS and single-jet spectra in hadron-nucleus collisions admit a description in terms of the same collective nuclear gluon density, albeit in the form of highly nonlinear quadratures. The universality classes introduced in [5,6] allow one to relate the nonlinearity properties of final states from different partonic pQCD subprocesses to the pattern of color flow from the incident parton to final-state dijet. A full derivation of nonlinear $k_\perp$ factorization for all high-energy single-jet spectra was published in [4]; the forward quark-antiquark dijet production in DIS and pion-nucleus collisions was studied in [2,3], respectively; the results for the two-particle spectrum of open heavy flavor production $g \to Q\overline{Q}$ in gluon-nucleus collisions—the dominant source of charm in proton-nucleus collisions—were presented in [5,6]; quark-gluon dijets in quark-nucleus interactions—the dominant source of forward dijets in the proton fragmentation region of proton-nucleus collisions—were treated in [6].

In this communication we report the derivation of nonlinear $k_\perp$ factorization for the last missing pQCD subprocess—the production of hard gluon-gluon dijets in gluon-nucleus collisions. As is well known, the density of soft (with respect to the beam proton) gluons is dominated by the splitting of gluons $g \to gg$; furthermore, as was shown in the classic works by Kuraev, Lipatov, and Fadin [9], in high-energy pQCD the dominant contribution to production processes comes from the so-called multiregge kinematics, i.e., the production of gluons or clusters of jets separated by large rapidity and with (reggeized) gluon exchange between clusters, beam, and target in the t channel. The corollary is that, in nucleon-nucleon collisions, the cross section for production of the central cluster of jets is $k_\perp$ factorizable in terms of the beam and target unintegrated gluon densities. The subject of this work is a change of the pattern of $k_\perp$ factorization from the free nucleon to a nuclear target at $x \lesssim x_A \approx 0.1 \cdot A^{-1/3}$ (for the definition of x_A for a target nucleus of mass number A see below), when the multiple gluon exchanges are coherently enhanced by the large thickness of the nucleus. Arguably, the linear $k_\perp$

*Electronic address: N. Nikolaev@fz-juelich.de
†Electronic address: Wo.Schaefer@fz-juelich.de
‡Electronic address: B.Zakharov@fz-juelich.de

 © 2005 The American Physical Society

factorization on the beam proton side will be retained for clusters of jets separated by a large rapidity from the beam and target partons, and we focus on the underlying pQCD subprocess $gA \to ggX$. At the not so high energies of the relativistic heavy ion collider (RHIC), the coherency condition can be met only in the proton (deuteron) fragmentation region of pA (dA) collisions, where the contribution from gluon-gluon dijets is marginal (see [10] and references therein). This subprocess will be a principal building block of the pQCD description of the midrapidity dijet production in pA collisions at the Large Hadron Collider (LHC), however. The incident gluon which enters the considered subprocess $gA \to ggX$ is only a part of the color-singlet projectile proton and carries a net color charge. Nonetheless, all partial cross sections for the excitation of the gluon-gluon dijets in all color representations are infrared finite. Furthermore, the effect of intranuclear interactions of beam spectator partons cancels out upon integration over the whole transverse phase space of spectator partons [11]. An explicit demonstration of such a cancellation for incident gluons carrying a small fraction of the energy of the projectile quark is found in Sec. II of Ref. [4].

The non-Abelian intranuclear evolution of gluon-gluon states is quite involved—at arbitrary number of colors N_c two gluons couple to seven irreducible representations. Based on the reduction of the dijet production problem to the interaction of color-singlet multiparton states with the nuclear target [2,6,11–13], we report an explicit form of evolution matrices for arbitrary N_c. We demonstrate how the forbidding case of seven-channel non-Abelian evolution equations can be diagonalized in an explicit form in the large-N_c approximation—this is reminiscent of our finding of the reduction of the three-channel non-Abelian evolution for quark-gluon dijets to a two-channel problem [6].

The close rapidity jets are of an obvious experimental interest, and we do not impose restrictions on the rapidity separation of jets in the dijet. The production of gluon-gluon dijets on nuclear targets in the limit of strong ordering of the rapidities of the produced gluons has been discussed earlier by several authors [14,15]. The starting points are similar, and in the limit of large rapidity separation of jets, our color-dipole representation for the fully inclusive digluon spectrum coincides with its counterpart for the contribution from the subprocess $gA \to ggX$ to the reaction $qA \to qggX$ studied in [14,15]. The difference is that Refs. [14,15] stop with a color-dipole representation for the dijet spectrum of the form which is equivalent to that obtained upon the application of our Sylvester expansion [2,6] for the four-parton S matrix and blocks further analytic derivations, so that Baier *et al.* resort to the brute force multidimensional numerical Fourier transform [15]. In contrast to that, our technique enables a derivation of the spectra of gluon-gluon dijets in all color representations in the form of explicit quadratures in terms of the collective nuclear unintegrated glue. As we commented in [6], our analytical results anticipated the trends of the nuclear decorrelation of dijets observed in the numerical studies of Ref. [15]. Our quadratures for the dijet spectra fully confirm our concept of universality classes [5,6]. For instance, the nonlinear $k_\perp$ factorization properties of excitation of digluons in higher color representations are the same as those in excitation of color-octet quark-antiquark dijets in DIS and quark-gluon dijets in higher color representations in qA collisions. We corroborate the point that the distinct properties of the initial and final-state interactions inherent to this universality class call upon the collective nuclear glue defined for slices of a nucleus. The only change from one pQCD subprocess to another is that they pick up different components of the color-density matrix for the nuclear glue. The processes of excitation of dijets in the same color multiplet as the incident parton, $g \to \{gg\}_8$, $g \to \{q\bar{q}\}_8$, $q \to \{qg\}_3$, share the representation in the form of the hard fragmentation of the scattered incident parton with the in-nucleus modified fragmentation function. The diffractive excitation of digluons in the antisymmetric octet is similar to diffractive excitation of color-triplet qg dijets in qA collisions and color-octet quark-antiquark dijets in gA collisions. In both $g \to gg$ and $q \to qg$ processes coherent diffractive excitation of incident partons with net color charge is suppressed by a nuclear absorption factor which can be identified with Bjorken's gap survival probability [16] (see, however, a special case of diffractive excitation $g \to \{q\bar{q}\}_8$, which vanishes to the leading order of large-N_c perturbation theory [5]).

The further presentation is organized as follows: We start with the discussion of the reaction kinematics and the master formula for the dijet cross section in Sec. II. The interaction properties of the two-gluon and three-gluon states are presented in Sec. III. The technically rather involved derivation of the nuclear S matrix for the four-gluon state is the subject of Sec. IV. In Sec. V we report the linear $k_\perp$ factorization formula for the gluon-gluon dijet cross section for the free-nucleon target. The principal new results of our study—nonlinear $k_\perp$ factorization formulas for gluon-gluon dijets in different color representations, their classification in universality classes, and a comparison to other dijet processes—are reported in Sec. VI. In Sec. VII section we summarize our main results.

The technicalities of the construction of the irreducible representations for the two-gluon states at an arbitrary number of colors N_c are reported in Appendices A and B. The exact integration of non-Abelian evolution equations for the four-gluon system and the derivation of explicit quadratures for the dijet spectrum is possible only for large N_c, although our results pave a way to a systematic calculation of higher order terms of $1/N_c$ perturbation theory [2]. On the other hand, the single-jet problem can be solved exactly at arbitrary N_c [4], and in Appendix C we show how the coupled seven-channel equations can be exactly diagonalized in the t-channel basis appropriate for the single-jet problem. In Appendix D we give a summary of different components of the color-density matrix for nuclear glue which enter the description of different pQCD subprocesses.

II. THE MASTER FORMULA FOR GLUON-GLUON DIJET PRODUCTION OFF FREE NUCLEONS AND NUCLEI

A. Kinematics and nuclear coherency

Our exposition of the master formula for dijet production follows closely our recent work on quark-gluon dijets [6].

To the lowest order in pQCD the underlying subprocess for gluon-gluon dijet production in the proton fragmentation region of proton-nucleus collisions is a collision of a gluon g^* from the proton with a gluon g_N from the target,

$$g^* g_N \to gg.$$

It is a pQCD Bremsstrahlung off a gluon tagged by the scattered gluon. We do not restrict ourselves to the emission of slow, $z \ll 1$ gluons. In the case of a nuclear target one has to deal with multiple gluon exchanges which are enhanced by a large thickness of the target nucleus.

From the laboratory, i.e., the nucleus rest frame, standpoint it can be viewed as an excitation of the perturbative $|gg\rangle$ Fock state of the physical projectile $|g^*\rangle$ by one-gluon exchange with the target nucleon or multiple gluon exchanges with the target nucleus. Here the collective nuclear effects develop, and the frozen impact parameter approximation holds, if the coherency over the thickness of the nucleus holds for the gg Fock states, i.e., if the coherence length l_c is larger than the diameter of the nucleus $2R_A$,

$$l_c = \frac{2E_{g^*}}{(Q^*)^2 + M_\perp^2} = \frac{1}{xm_N} > 2R_A, \tag{1}$$

where

$$M_\perp^2 = \frac{\boldsymbol{p}_1^2}{z_1} + \frac{\boldsymbol{p}_2^2}{z_2} \tag{2}$$

is the transverse mass squared of the gg state, $\boldsymbol{p}_{1,2}$ and $z_{1,2}$ are the transverse momenta and fractions of the incident gluon's momentum carried by the outgoing gluon one and gluon two, respectively, $(z_1 + z_2 = 1)$, and E_{g^*} is the energy of the beam gluon g^* in the target rest frame. The virtuality of the incident gluon g^* equals $(Q^*)^2 = (\boldsymbol{p}^*)^2$, where $\boldsymbol{p}^*$ is the transverse momentum of g^* in the incident proton (Fig. 1). In the antilaboratory (Breit) frame, partons with a momentum xp_N have a longitudinal localization of the order of their Compton wavelength $\lambda = 1/xp_N$, where

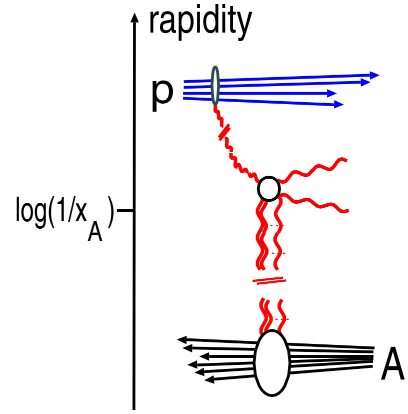

FIG. 1 (color online). The rapidity structure of the radiation of gluons by gluons $g \to gg$ in the nuclear coherency region of pA collisions.

p_N is the momentum per nucleon. The coherency over the thickness of the nucleus in the target rest frame is equivalent to the spatial overlap of parton fields of different nucleons at the same impact parameter in the Lorentz-contracted ultrarelativistic nucleus. In the overlap regime one would think of the fusion of partons form different nucleons and collective nuclear parton densities [17]. The overlap takes place if λ exceeds the Lorentz-contracted thickness of the ultrarelativistic nucleus,

$$\lambda = \frac{1}{xp_N} > 2R_A \cdot \frac{m_N}{p_N}, \tag{3}$$

which is identical to the condition (1).

Qualitatively, both descriptions of collective nuclear effects are equivalent to each other. Quantitatively, the laboratory frame approach takes advantage of the well-developed multiple-scattering theory of interactions of color dipoles with nuclei [2,18–20]. From the practical point of view, the coherency condition $x < x_A$ restricts collective effects in hard processes at RHIC to the proton fragmentation region of pA, dA collisions, but at LHC our treatment will hold down to the midrapidity region of pA collisions. The target frame rapidity structure of the considered $g^* \to gg$ excitation is shown in Fig. 1. The (pseudo)rapidities of the final-state partons must satisfy $\eta_{1,2} > \eta_A = \log 1/x_A$. The rapidity separation of the two hard gluon jets,

$$\Delta\eta_{gg} = \log\frac{z_2}{z_1}, \tag{4}$$

is considered to be finite. Both jets are supposed to be separated by a large rapidity from other jets in the beam hemisphere or in the target nucleus hemisphere; the gaps between all jets, beam spectators, and target debris are filled by soft hadrons from an underlying event. As was explained in the introduction, our results will be a building block of the pQCD description of midrapidity to proton-hemisphere dijets in pA collisions at LHC.

B. Master formula for excitation of gluon-gluon dijets

In the nucleus rest frame, relativistic partons g^*, g_1 and g_2 propagate along straightline, fixed-impact parameter trajectories. To the lowest order in pQCD the Fock state expansion for the physical state $|g^*\rangle_{\rm phys}$ reads

$$|g^*\rangle_{\rm phys} = |g^*\rangle_0 + \Psi(z_1, \boldsymbol{r})|gg\rangle_0, \quad (5)$$

where $\Psi(z_1, \boldsymbol{r})$ is the probability amplitude to find the gg system with the separation $\boldsymbol{r}$ in the two-dimensional impact parameter space, the subscript 0 refers to bare partons. The perturbative coupling of the $g^* \to gg$ transition is reabsorbed into the light cone wave function $\Psi(z_1, \boldsymbol{r})$. We also omitted a wave function renormalization factor, which is of no relevance for the inelastic excitation to the perturbative order discussed here. The explicit expression for $\Psi(z_1, \boldsymbol{r})$ in terms of the gluon-splitting function and the gluon virtuality $(Q^*)^2$ will be presented below. For the sake of simplicity we take the collision axis along the momentum of the incident quark g^*; the transformation between the transverse momenta in the g^*-target and p-target reference frames is trivial [4].

If $\boldsymbol{b}$ is the impact parameter of the projectile g^*, then

$$\boldsymbol{b}_1 = \boldsymbol{b} - z_2\boldsymbol{r}, \qquad \boldsymbol{b}_2 = \boldsymbol{b} + z_1\boldsymbol{r}. \quad (6)$$

By the conservation of impact parameters, the action of the S matrix on $|g^*\rangle_{\rm phys}$ takes a simple form

$$\begin{aligned}\mathsf{S}|g^*\rangle_{\rm phys} &= \mathsf{S}_g(\boldsymbol{b})|g^*\rangle_0 + \mathsf{S}_g(\boldsymbol{b}_1)\mathsf{S}_g(\boldsymbol{b}_2)\Psi(z_1, \boldsymbol{r})|gg\rangle_0 \\ &= \mathsf{S}_g(\boldsymbol{b})|g^*\rangle_{\rm phys} + [\mathsf{S}_g(\boldsymbol{b}_1)\mathsf{S}_g(\boldsymbol{b}_2) - \mathsf{S}_g(\boldsymbol{b})] \\ &\quad \times \Psi(z_1, \boldsymbol{r})|gg\rangle_0. \end{aligned} \quad (7)$$

Here we explicitly decomposed the final state into the (quasi)elastically scattered $|g^*\rangle_{\rm phys}$ and the excited state $|gg\rangle_0$. The two terms in the latter describe a scattering on the target of the gg system formed way in front of the target and the transition $g^* \to gg$ after the interaction of the state $|g^*\rangle_0$ with the target, as illustrated in Fig. 2. The contribution from transitions $g^* \to gg$ inside the target nucleus vanishes in the high-energy limit of $x \lesssim x_A$.[1] We recall that the s-channel helicity of all gluons is conserved.

The probability amplitude for the two-jet spectrum is given by the Fourier transform

$$\int d^2\boldsymbol{b}_1 d^2\boldsymbol{b}_2 \exp[-i(\boldsymbol{p}_1\boldsymbol{b}_1 + \boldsymbol{p}_2\boldsymbol{b}_2)] \times [\mathsf{S}_g(\boldsymbol{b}_1)\mathsf{S}_g(\boldsymbol{b}_2) - \mathsf{S}_g(\boldsymbol{b})]\Psi(z_1, \boldsymbol{r}). \quad (8)$$

The differential cross section is proportional to the modulus squared of (8),

$$\begin{aligned}&\int d^2\boldsymbol{b}'_1 d^2\boldsymbol{b}'_2 \exp[i(\boldsymbol{p}_1\boldsymbol{b}'_1 + \boldsymbol{p}_2\boldsymbol{b}'_2)][\mathsf{S}^\dagger_g(\boldsymbol{b}'_1)\mathsf{S}^\dagger_g(\boldsymbol{b}'_2) - \mathsf{S}^\dagger_g(\boldsymbol{b}')] \\ &\times \Psi^*(z_1, \boldsymbol{r}') \int d^2\boldsymbol{b}_1 d^2\boldsymbol{b}_2 \exp[-i(\boldsymbol{p}_1\boldsymbol{b}_1 + \boldsymbol{p}_2\boldsymbol{b}_2)] \\ &\times [\mathsf{S}_g(\boldsymbol{b}_1)\mathsf{S}_g(\boldsymbol{b}_2) - \mathsf{S}_g(\boldsymbol{b})]\Psi(z_1, \boldsymbol{r}). \end{aligned} \quad (9)$$

The crucial point is that the Hermitian conjugate $\mathsf{S}^\dagger$ can be viewed as the S matrix for an antiparton [2,11,12]. Consequently, the four terms in the product

$$[\mathsf{S}_g(\boldsymbol{b}'_1)\mathsf{S}_g(\boldsymbol{b}'_2) - \mathsf{S}_g(\boldsymbol{b}')]^\dagger[\mathsf{S}_g(\boldsymbol{b}_1)\mathsf{S}_g(\boldsymbol{b}_2) - \mathsf{S}_g(\boldsymbol{b})]$$

admit a simple interpretation:

$$\mathsf{S}^{(2)}_{g^{*\prime}g^*}(\boldsymbol{b}', \boldsymbol{b}) = \mathsf{S}^\dagger_g(\boldsymbol{b}')\mathsf{S}_g(\boldsymbol{b}) \quad (10)$$

can be viewed as a S matrix for elastic scattering on a target of the $g^{*\prime}g^*$ state in which the (anti)gluon $g^{*\prime}$ propagates at the impact parameter $\boldsymbol{b}'$. The averaging over the color states of the beam parton g^* amounts to the dipole g^*g^* being in the color-singlet state. Similarly,

$$\begin{aligned}\mathsf{S}^{(3)}_{g^{*\prime}g_1g_2}(\boldsymbol{b}', \boldsymbol{b}_1, \boldsymbol{b}_2) &= \mathsf{S}^\dagger_g(\boldsymbol{b}')\mathsf{S}_g(\boldsymbol{b}_1)\mathsf{S}_g(\boldsymbol{b}_2), \\ \mathsf{S}^{(3)}_{g'_1g'_2g^*}(\boldsymbol{b}, \boldsymbol{b}'_1, \boldsymbol{b}'_2) &= \mathsf{S}^\dagger_g(\boldsymbol{b}'_1)\mathsf{S}^\dagger_g(\boldsymbol{b}'_2)\mathsf{S}_g(\boldsymbol{b}), \\ \mathsf{S}^{(4)}_{g'_1g'_2g_1g_2}(\boldsymbol{b}'_1, \boldsymbol{b}'_2, \boldsymbol{b}_1, \boldsymbol{b}_2) &= \mathsf{S}^\dagger_g(\boldsymbol{b}'_1)\mathsf{S}^\dagger_g(\boldsymbol{b}'_2)\mathsf{S}_g(\boldsymbol{b}_1)\mathsf{S}_g(\boldsymbol{b}_2). \end{aligned} \quad (11)$$

describe elastic scattering on a target of the overall color-singlet three- and four-gluon states, respectively. This is shown schematically in Fig. 3. Here we suppressed the matrix elements of $\mathsf{S}^{(n)}$ over the target nucleon; full details of the derivation based on the Glauber-Gribov multiple-scattering theory for nuclear targets [21,22] and the closure relation are found in [2]. Specifically, in the calculation of the inclusive cross sections one averages over the color states of the beam gluon g, sums over color states X of final-state gluons g_1, g_2, takes the matrix products of $\mathsf{S}^\dagger$ and S with respect to the relevant color indices entering $\mathsf{S}^{(n)}$ and sums over all nuclear final states applying the closure relation. The technicalities of the derivation of $\mathsf{S}^{(n)}$ will be presented below; here we cite the master formula for the dijet cross section, which is the Fourier transform of the two-body density matrix:

$$\begin{aligned}\frac{d\sigma(g^* \to g_1g_2)}{dzd^2\boldsymbol{p}_1d^2\boldsymbol{p}_2} = \frac{1}{(2\pi)^4} &\int d^2\boldsymbol{b}_1 d^2\boldsymbol{b}_2 d^2\boldsymbol{b}'_1 d^2\boldsymbol{b}'_2 \\ &\times \exp[-i\boldsymbol{p}_2(\boldsymbol{b}_2 - \boldsymbol{b}'_2) - i\boldsymbol{p}_1(\boldsymbol{b}_1 - \boldsymbol{b}'_1)] \\ &\times \Psi(z_1, \boldsymbol{b}_1 - \boldsymbol{b}_2)\Psi^*(z_1, \boldsymbol{b}'_1 - \boldsymbol{b}'_2) \quad (12)\end{aligned}$$

$$\begin{aligned}&\sum_X \langle X|\{\mathsf{S}^{(4)}_{g'_1g'_2g_1g_2}(\boldsymbol{b}'_1, \boldsymbol{b}'_2, \boldsymbol{b}_1, \boldsymbol{b}_2) + \mathsf{S}^{(2)}_{g^{*\prime}g^*}(\boldsymbol{b}', \boldsymbol{b}) \\ &- \mathsf{S}^{(3)}_{g'_1g'_2g^*}(\boldsymbol{b}, \boldsymbol{b}'_1, \boldsymbol{b}'_2) - \mathsf{S}^{(3)}_{g^{*\prime}g_1g_2}(\boldsymbol{b}', \boldsymbol{b}_1, \boldsymbol{b}_2)\}|in\rangle.\end{aligned}$$

[1] In terms of the light cone approach to the QCD Landau-Pomeranchuk-Migdal effect, this corresponds to the thin-target limit [13].

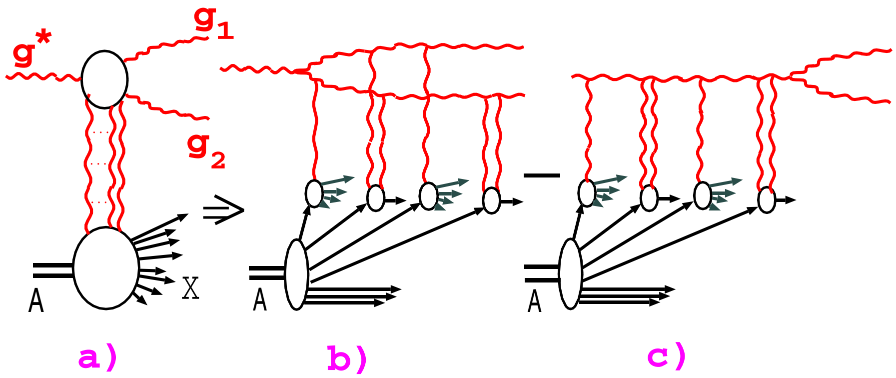

FIG. 2 (color online). Typical contribution to the excitation amplitude for $gA \to g_1 g_2 X$, with multiple color excitations of the nucleus. The amplitude receives contributions from processes that involve interactions with the nucleus after and before the virtual decay which interfere destructively.

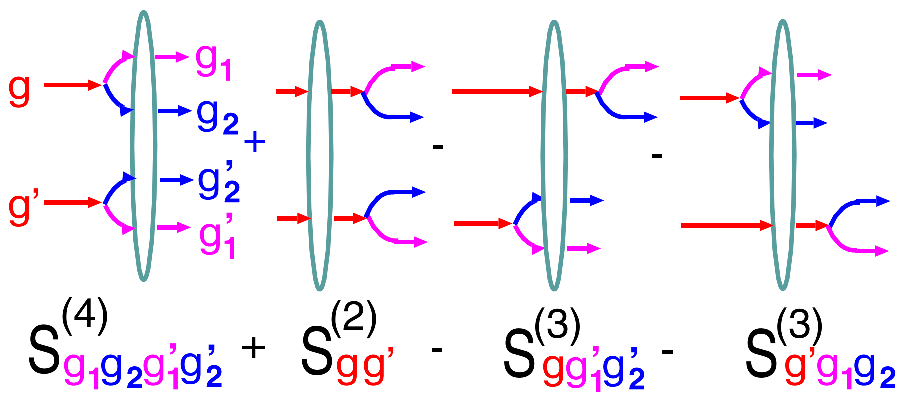

FIG. 3 (color online). The S-matrix structure of the two-body density matrix for excitation $g \to g_1 g_2$.

Hereafter, we describe the final-state dijet in terms of the jet momentum $\boldsymbol{p} \equiv \boldsymbol{p}_1$, $z \equiv z_1$, and the decorrelation (acoplanarity) momentum $\boldsymbol{\Delta} = \boldsymbol{p}_1 + \boldsymbol{p}_2$. We also introduce

$$\boldsymbol{s} = \boldsymbol{b}_2 - \boldsymbol{b}_2', \tag{13}$$

in terms of which $\boldsymbol{b}_1 - \boldsymbol{b}_1' = \boldsymbol{s} + \boldsymbol{r} - \boldsymbol{r}'$ and

$$\exp[-i\boldsymbol{p}_2(\boldsymbol{b}_2 - \boldsymbol{b}_2') - i\boldsymbol{p}_1(\boldsymbol{b}_1 - \boldsymbol{b}_1')] = \exp[-i\boldsymbol{\Delta}\boldsymbol{s} - i\boldsymbol{p}\boldsymbol{r} + i\boldsymbol{p}\boldsymbol{r}'], \tag{14}$$

so that the dipole parameter $\boldsymbol{s}$ is conjugate to the acoplanarity momentum $\boldsymbol{\Delta}$.

III. CALCULATION OF THE 2-PARTON AND 3-PARTON S MATRICES

A. The gluon-nucleon S matrix and the $k_\perp$ factorization representations for the color-dipole cross section

In order to set up the formalism, we start with the S-matrix representation for the cross section of interaction of the gg color dipole with the free-nucleon target. To the two-gluon-exchange approximation, the S matrix of the gluon-nucleon interaction equals

$$\mathsf{S}_N(\boldsymbol{b}) = \mathbb{1} + iT^a V_a \chi(\boldsymbol{b}) - \tfrac{1}{2} T^a T^a \chi^2(\boldsymbol{b}), \tag{15}$$

where T^a is the $SU(N_c)$ generator in the adjoint representation, $\langle g^b | T^a | g^c \rangle = -i f_{abc}$, and $T^a V_a \chi(\boldsymbol{b})$ is the gluon-nucleon eikonal for single gluon exchange. The vertex V_a for excitation of the nucleon $g^a N \to N_a^*$ into a color-octet state is so normalized that after application of closure over the final-state excitations N^* the vertex $g^a g^b NN$ equals $\langle N | V_a^\dagger V_b | N \rangle = \delta_{ab}$. The second order term in (15) already uses this normalization. The S matrix of the gg-nucleon interaction equals

$$\mathsf{S}_{gg}^{(2)}(\boldsymbol{b}_1, \boldsymbol{b}_2) = \frac{\langle N | \mathrm{Tr}[\mathsf{S}_N(\boldsymbol{b}_1)\mathsf{S}_N^\dagger(\boldsymbol{b}_2)] | N \rangle}{\langle N | \mathrm{Tr}\mathbb{1} | N \rangle}. \tag{16}$$

The corresponding profile function is $\Gamma_2(\boldsymbol{b}_1, \boldsymbol{b}_2) = 1 - \mathsf{S}_{gg}^{(2)}(\boldsymbol{b}_1, \boldsymbol{b}_2)$. The dipole cross section for interaction of the color-singlet gg dipole $\boldsymbol{r} = \boldsymbol{b}_1 - \boldsymbol{b}_2$ with the free nucleon is obtained upon the integration over the overall impact parameter

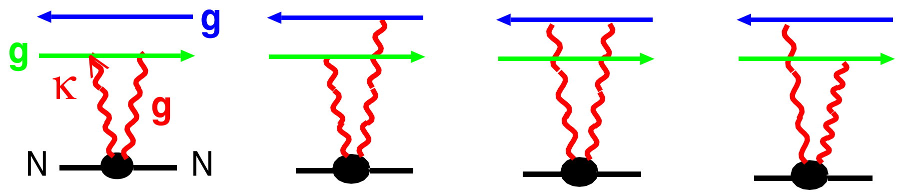

FIG. 4 (color online). The four Feynman diagrams for the gluon-gluon dipole-nucleon interaction by the two-gluon pomeron exchange in the t channel.

$$\sigma(\boldsymbol{r}) = 2\int d^2\boldsymbol{b}_1 \Gamma_2(\boldsymbol{b}_1, \boldsymbol{b}_1 - \boldsymbol{r}) = C_A \int d^2\boldsymbol{b}_1[\chi(\boldsymbol{b}_1) - \chi(\boldsymbol{b}_1 - \boldsymbol{r})]^2, \quad (17)$$

where $C_A = T^a T^a = N_c$ is the gluon Casimir operator. Equation (17) sums up the contributions from the four Feynman diagrams of Fig. 4 and is related to the gluon density in the target by the $k_\perp$ factorization formula [20,23]

$$\sigma(x, \boldsymbol{r}) = \frac{C_A}{C_F}\int d^2\boldsymbol{\kappa} f(x, \boldsymbol{\kappa})[1 - \exp(i\boldsymbol{\kappa}\boldsymbol{r})], \quad (18)$$

where $C_F = (N_c^2 - 1)/2N_c$ is the quark Casimir. Recall that the unintegrated gluon density

$$\mathcal{F}(x, \kappa^2) = \frac{\partial G(x, \kappa^2)}{\partial \log \kappa^2} \quad (19)$$

was defined with respect to the $q\bar{q}$ color-dipole probe and is related to $f(x, \boldsymbol{\kappa})$ through

$$f(x, \boldsymbol{\kappa}) = \frac{4\pi\alpha_S(r)}{N_c}\cdot\frac{1}{\kappa^4}\cdot\mathcal{F}(x, \kappa^2). \quad (20)$$

Hereafter, we suppress the variable x in the gluon densities and dipole cross sections. The energy dependence of the dipole cross section is governed by the color-dipole leading $\log\frac{1}{x}$ evolution [20,24], the related evolution for the unintegrated gluon density is described by the familiar momentum-space BFKL (Balitsky-Fadin-Kuraev-Lipatov) equation [9,25].

The S matrix for coherent interaction of the color dipole with the nuclear target is given by the Glauber-Gribov formula [21,22]

$$\mathsf{S}[\boldsymbol{b}, \sigma(\boldsymbol{r})] = \exp[-\tfrac{1}{2}\sigma(\boldsymbol{r})T(\boldsymbol{b})], \quad (21)$$

where

$$T(\boldsymbol{b}) = \int_{-\infty}^{\infty} dr_z n_A(\boldsymbol{b}, r_z) \quad (22)$$

is the optical thickness of the nucleus. The nuclear density $n_A(\boldsymbol{b}, r_z)$ is normalized according to $\int d^3\vec{r} n_A(\boldsymbol{b}, r_z) = \int d^2\boldsymbol{b} T(\boldsymbol{b}) = A$, where A is the nuclear mass number.

In the specific case of $\mathsf{S}^{(2)}_{g^*g^*}(\boldsymbol{b}', \boldsymbol{b})$ the color dipole equals

$$\boldsymbol{r}_{gg} = \boldsymbol{b} - \boldsymbol{b}' = \boldsymbol{s} + z\boldsymbol{r} - z\boldsymbol{r}', \quad (23)$$

and $\mathsf{S}^{(2)}_{g^*g^*}(\boldsymbol{b}', \boldsymbol{b})$ entering Eq. (12) will be given by the Glauber-Gribov formula

$$\mathsf{S}^{(2)}_{g^*g^*}(\boldsymbol{b}', \boldsymbol{b}) = \mathsf{S}[\boldsymbol{b}, \sigma(\boldsymbol{s} + z\boldsymbol{r} - z\boldsymbol{r}')]. \quad (24)$$

B. The S matrix for the color-singlet ggg system

Here, there are two possibilities to couple three gluons to a color singlet, but only the f coupling is relevant to our problem; see also Appendices A, B, and C.

For the generic three-gluon state shown in Fig. 5 the color-dipole cross section equals

$$\sigma^{(3)}(\boldsymbol{b}_1, \boldsymbol{b}_2, \boldsymbol{b}_3) = \tfrac{1}{2}[\sigma(\boldsymbol{r}_{12}) + \sigma(\boldsymbol{r}_{23}) + \sigma(\boldsymbol{r}_{31})], \quad (25)$$

where $\boldsymbol{r}_{ik} = \boldsymbol{b}_k - \boldsymbol{b}_i$. The configuration of color dipoles for the case of our interest is shown in Fig. 5 (see the related derivation in [11]). For the $g'g_1g_2$ state the relevant dipole sizes in (25) equal

$$\boldsymbol{r}_{g_1g^{*\prime}} = \boldsymbol{b}_1 - \boldsymbol{b}' = \boldsymbol{s} - z\boldsymbol{r}, \qquad \boldsymbol{r}_{g_1g_2} = \boldsymbol{b}_2 - \boldsymbol{b}_1 = \boldsymbol{r}, \qquad \boldsymbol{r}_{g^{*\prime}g_2} = \boldsymbol{b}' - \boldsymbol{b}_2 = \boldsymbol{s} + \boldsymbol{r} - z\boldsymbol{r}', \quad (26)$$

so that

$$\sigma_{g^{*\prime}g_1g_2} = \tfrac{1}{2}[\sigma(\boldsymbol{r}) + \sigma(\boldsymbol{s} + \boldsymbol{r} - z\boldsymbol{r}') + \sigma(\boldsymbol{s} - z\boldsymbol{r}')],$$
$$\sigma_{g^*g_1'g_2'} = \tfrac{1}{2}[\sigma(-\boldsymbol{r}') + \sigma(\boldsymbol{s} - \boldsymbol{r}' + z\boldsymbol{r}) + \sigma(\boldsymbol{s} + z\boldsymbol{r})]. \quad (27)$$

The overall color-singlet three-gluon state has a unique color structure and its elastic scattering on a nucleus is a

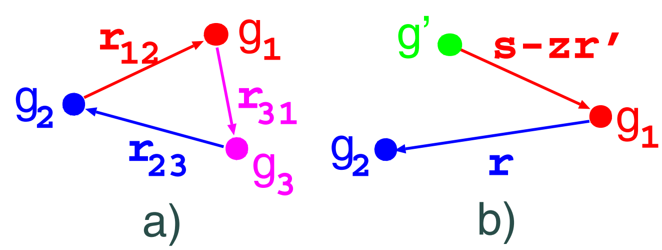

FIG. 5 (color online). The color-dipole structure of (a) the generic 3-gluon system of dipoles and (b) of the $g'g_1g_2$ system which emerges in the S-matrix structure of the two-body density matrix for excitation $g \to g_1g_2$.

single-channel problem. Consequently, the nuclear S matrix is given by the single-channel Glauber-Gribov formula

$$\begin{aligned} \mathsf{S}^{(3)}_{g^{*\prime}g_1g_2}(\boldsymbol{b}, \boldsymbol{b}'_q, \boldsymbol{b}'_g) &= \mathsf{S}[\boldsymbol{b}, \sigma_{g^{*\prime}g_1g_2}], \\ \mathsf{S}^{(3)}_{g^{*\prime}g'_1g'_2}(\boldsymbol{b}', \boldsymbol{b}_q, \boldsymbol{b}_g) &= \mathsf{S}[\boldsymbol{b}, \sigma_{g^{*}g'_1g'_2}]. \end{aligned} \tag{28}$$

IV. DIPOLE CROSS SECTION OPERATOR FOR FOUR-GLUON STATES

We now come to the major technical novelty of this paper, the dipole cross section matrix for the four-gluon system. Here, as in the previous applications for $qq\bar{q}\,\bar{q}$ and $q\bar{q}gg$ systems, the large N_c limit offers a particularly useful expansion. We thus discuss the general case in which the gluon is transforming in the adjoint representation of $SU(N_c)$. In order to construct the relevant four-gluon states, our first task is to decompose the product states of the adjoint $\times$ adjoint system into irreducible representations. The adjoint (or regular) representation of $SU(N_c)$ has $N_c^2 - 1$ states, and the Clebsch-Gordan series for the product of two adjoints reads

$$\begin{aligned} (N_c^2-1)\times(N_c^2-1) &= 1 + (N_c^2-1)_A + (N_c^2-1)_S + \frac{(N_c^2-4)(N_c^2-1)}{4} + \left[\frac{(N_c^2-4)(N_c^2-1)}{4}\right]^* \\ &\quad + \frac{N_c^2(N_c+3)(N_c-1)}{4} + \frac{N_c^2(N_c-3)(N_c+1)}{4} \\ &= 1 + 8_A + 8_S + 10 + \overline{10} + 27 + R_7. \end{aligned} \tag{29}$$

In the last line, we named the representations by their $SU(3)$ dimensions, except for one of the symmetric representations that vanishes for $N_c = 3$ and will be referred to as R_7.

A. Projection operators onto irreducible representations

The derivation of projectors onto the representations (29) is a lengthy, though standard, exercise [26]. While in our earlier solution of the analogous problem for the $qgg\bar{q}$ system it had proven convenient to represent gluons in a double line notation as pointlike quark-antiquark systems, here we find it expedient to stick to purely adjoint-index tensors. We present here a sketch of the construction of irreducible representations (29); the details are given in Appendices A and B.

If $t^a, a = 1\dots N_c^2 - 1$ are $SU(N_c)$ generators in the fundamental representation, the familiar f and d tensors are defined through

$$t^a t^b = \frac{1}{2N_c}\delta_{ab}\mathbb{1} + \frac{1}{2}(d_{abc} + if_{abc})t^c, \tag{30}$$

and $T^a_{bc} = -if_{abc}$ are the $SU(N_c)$ generators in the adjoint representation.

First we decompose the product representation space into its symmetric and antisymmetric parts, respectively:

$$\mathbb{1}^{\,ab}_{\,cd} \equiv \delta_{ac}\delta_{bd} = S^{ab}_{cd} + \mathcal{A}^{ab}_{cd}, \tag{31}$$

where

$$\begin{aligned} S^{ab}_{cd} &\equiv \tfrac{1}{2}(\delta_{ac}\delta_{bd} + \delta_{ad}\delta_{bc}), \\ \mathcal{A}^{ab}_{cd} &\equiv \tfrac{1}{2}(\delta_{ac}\delta_{bd} - \delta_{ad}\delta_{bc}). \end{aligned} \tag{32}$$

The complex

$$iY^{ab}_{cd} \equiv \frac{i}{2}(d_{adk}f_{kbc} + f_{adk}d_{kbc}) \tag{33}$$

as well as

$$\begin{aligned} [D_t]^{ab}_{cd} \equiv d_{ack}d_{kbd}, \qquad [D_u]^{ab}_{cd} \equiv d_{adk}d_{kbc}, \\ [D_s]^{ab}_{cd} \equiv d_{abk}d_{kcd} \end{aligned} \tag{34}$$

also prove helpful. All the above defined tensors S, $\mathcal{A}$, iY, D_s, D_t, D_u are Hermitian.

The $SU(N_c)$ projectors into the three lowest dimensional multiplets have manifestly the same form as their well-known $N_c = 3$ counterparts:

$$P[1]^{ab}_{cd} = \frac{1}{N_c^2-1}\delta_{ab}\delta_{cd}, \tag{35}$$

$$P[8_A]^{ab}_{cd} = \frac{1}{N_c}f_{abk}f_{kcd} = \frac{1}{N_c}if_{abk}if_{kdc}, \tag{36}$$

$$P[8_S]^{ab}_{cd} = \frac{N_c}{N_c^2-4}d_{abk}d_{kcd} = \frac{N_c}{N_c^2-4}[D_s]^{ab}_{cd}. \tag{37}$$

For the construction of higher multiplets a useful quantity is $Q^{cd}_{ab} = 4\cdot\mathrm{Tr}[t^a t^d t^b t^c]$, which, with indices suppressed, equals

$$Q = \frac{1}{N_c}(2S - (N_c^2-1)P[1]) + \frac{1}{2}(D_t + D_u - D_s) + iY. \tag{38}$$

Then, the crucial observation is [26] that

$$\mathbb{1} - Q^2 = \frac{N_c^2-1}{N_c}P[1] + \frac{N_c^2-4}{N_c}P[8_S] - P[8_A]. \tag{39}$$

Apparently in the subspaces that are projected onto by

$$S_\perp = S - P[1] - P[8_S], \qquad \mathcal{A}_\perp = \mathcal{A} - P[8_A], \tag{40}$$

the operator $\mathbb{1} - Q^2 = (\mathbb{1} + Q)(\mathbb{1} - Q)$ vanishes and Q has eigenvalues ± 1. We can thus write down projection operators that decompose $S_\perp$, $\mathcal{A}_\perp$ further, as

$$P^{\pm}_{A_\perp} = \tfrac{1}{2}(\mathbb{1} \pm Q)\mathcal{A}_\perp, \qquad P^{\pm}_{S_\perp} = \tfrac{1}{2}(\mathbb{1} \pm Q)S_\perp. \tag{41}$$

Checking how many states are contained in $P^{\pm}_{A_\perp}$, $P^{\pm}_{S_\perp}$, one may identify that $P^{+}_{A_\perp} = P[10]$, $P^{-}_{A_\perp} = P[\overline{10}]$, $P^{+}_{S_\perp} = P[27]$, and $P^{-}_{A_\perp} = P[R_7]$. In convenient form, with all indices shown again, they read:

$$\begin{aligned} P[10]^{ab}_{cd} &= \tfrac{1}{2}(\mathcal{A}^{ab}_{cd} - P[8_A]^{ab}_{cd} + iY^{ab}_{cd}), \\ P[\overline{10}]^{ab}_{cd} &= \tfrac{1}{2}(\mathcal{A}^{ab}_{cd} - P[8_A]^{ab}_{cd} - iY^{ab}_{cd}). \end{aligned} \tag{42}$$

$$\begin{aligned} P[27]^{ab}_{cd} = \frac{1}{2N_c}\Big(&(N_c+2)S^{ab}_{cd} - (N_c+2)(N_c-1)P[1]^{ab}_{cd} \\ &- \frac{1}{2}(N_c-2)(N_c+4)P[8_S]^{ab}_{cd} \\ &+ \frac{N_c}{2}([D_t]^{ab}_{cd} + [D_u]^{ab}_{cd})\Big), \end{aligned} \tag{43}$$

$$\begin{aligned} P[R_7]^{ab}_{cd} = \frac{1}{2N_c}\Big(&(N_c-2)S^{ab}_{cd} + (N_c-2)(N_c+1)P[1]^{ab}_{cd} \\ &+ \frac{1}{2}(N_c+2)(N_c-4)P[8_S]^{ab}_{cd} \\ &- \frac{N_c}{2}([D_t]^{ab}_{cd} + [D_u]^{ab}_{cd})\Big). \end{aligned} \tag{44}$$

It is now a simple matter to obtain the quadratic Casimirs (i.e. color charge squared) of the individual multiplets, which can be found in Table I.

B. Multigluon states

The above given projectors can be used to construct the color-space wave function of the multigluon states relevant for us. The four gluons have to be in a total color singlet, and all possible states are exhausted by coupling a chosen pair of gluons to all possible multiplets and the remaining two to an antimultiplet. The choice of pairs is of course arbitrary. Because averaging over colors of the incoming gluon amounts to the initial state

$$|\mathrm{in}\rangle = \frac{1}{\sqrt{N_c^2-1}}|8_A 8_A\rangle, \tag{45}$$

a convenient choice is the s-channel pairing

$$\begin{aligned} |R\overline{R}\rangle &\equiv |\{[g^a(\boldsymbol{b}_1)\otimes g^b(\boldsymbol{b}_2)]_R \otimes [g^c(\boldsymbol{b}_1')\otimes g^d(\boldsymbol{b}_2')]_{\overline{R}}\}_1\rangle \\ &= \frac{1}{\sqrt{\dim[R]}} P[R]^{ab}_{cd} |g^a(\boldsymbol{b}_1)\otimes g^b(\boldsymbol{b}_2)\otimes g^c(\boldsymbol{b}_1')\otimes g^d(\boldsymbol{b}_2')\rangle. \end{aligned} \tag{46}$$

The basis of color-singlet four-gluon states which contribute to the non-Abelian evolution of gluon-gluon dijets in our problem consists of $|11\rangle$, $|8_A8_A\rangle$, $|8_S8_S\rangle$, $|10\overline{10}\rangle$, $|\overline{10}10\rangle$, $|2727\rangle$, $|R_7R_7\rangle$. The mixed-symmetry color-singlet states like $|8_A8_S\rangle$ are possible but decouple from the above states.

We note in passing that the single-jet spectrum derives from the dijet spectrum by integration over all $\boldsymbol{\Delta}$, which entails $\boldsymbol{s} = 0$. For studying the transition from the dijet to single-jet problem an alternative, t-channel, pairing of gluons, (g_1g_1') and (g_2g_2'), proves to be a more convenient one. Evidently, the multiparton S matrices for different choices are related by a trivial permutation of the gluon impact parameters. For the reference purposes, in Appendix C we demonstrate how the coupled seven-channel problem is exactly diagonalized for the color-dipole configuration appropriate to the single-jet problem.

C. Multiparton S matrix and the four-body color-dipole cross section operator for the free-nucleon target

The frozen impact parameter approximation leads to a four-gluon S matrix of the form

$$\mathsf{S}^{(4)}_N(\boldsymbol{b}_1, \boldsymbol{b}_2, \boldsymbol{b}_1', \boldsymbol{b}_2') = \mathsf{S}_N(\boldsymbol{b}_1)\otimes \mathsf{S}_N(\boldsymbol{b}_2)\otimes \mathsf{S}_N(\boldsymbol{b}_1') \otimes \mathsf{S}_N(\boldsymbol{b}_2'). \tag{47}$$

Then, upon using Eq. (15), on a color-singlet four-particle state, the S matrix $\mathsf{S}^{(4)}_N$ takes the form

TABLE I. Properties of multiplets.

	symmetric				antisymmetric		
Name of rep.	1	8_S	27	R_7	8_A	10	$\overline{10}$
Dimension	1	N_c^2-1	$\frac{N_c^2(N_c+3)(N_c-1)}{4}$	$\frac{N_c^2(N_c-3)(N_c+1)}{4}$	N_c^2-1	$\frac{(N_c^2-4)(N_c^2-1)}{4}$	$\frac{(N_c^2-4)(N_c^2-1)}{4}$
Casimir $C_2[R]$	0	N_c	$2(N_c+1)$	$2(N_c-1)$	N_c	$2N_c$	$2N_c$
$\lambda_R = 1 - \frac{C_2[R]}{2C_A}$	1	$\frac{1}{2}$	$-\frac{1}{N_c}$	$\frac{1}{N_c}$	$\frac{1}{2}$	0	0

$$\begin{aligned}\mathsf{S}_N^{(4)}(\boldsymbol{b}_1, \boldsymbol{b}_2, \boldsymbol{b}'_1, \boldsymbol{b}'_2) &= 1 - \tfrac{1}{2}[T_1^a\chi(\boldsymbol{b}_1) + T_2^a\chi(\boldsymbol{b}_2) + T_{1'}^a\chi(\boldsymbol{b}'_1) + T_{2'}^a\chi(\boldsymbol{b}'_2)]^2 \\ &= 1 - \tfrac{1}{2}C_A[\chi^2(\boldsymbol{b}_1) + \chi^2(\boldsymbol{b}_2) + \chi^2(\boldsymbol{b}'_1) + \chi^2(\boldsymbol{b}'_2)] - T_1^aT_2^a\chi(\boldsymbol{b}_1)\chi(\boldsymbol{b}_2) - T_{1'}^aT_{2'}^a\chi(\boldsymbol{b}'_1)\chi(\boldsymbol{b}'_2) \\ &\quad - T_2^aT_{1'}^a\chi(\boldsymbol{b}_2)\chi(\boldsymbol{b}'_1) - T_1^aT_{2'}^a\chi(\boldsymbol{b}_1)\chi(\boldsymbol{b}'_2) - T_1^aT_{1'}^a\chi(\boldsymbol{b}_1)\chi(\boldsymbol{b}'_1) - T_2^aT_{2'}^a\chi(\boldsymbol{b}_2)\chi(\boldsymbol{b}'_2). \end{aligned} \quad (48)$$

Here products like $T_1^aT_{2'}^a$ are shorthands for $T^a \otimes 1 \otimes 1 \otimes T^a$, what acts in the space spanned by gluon states $g_1^a \otimes g_2^b \otimes g_{1'}^c \otimes g_{2'}^d$.

In the following we shall heavily exploit the color-singlet condition for the four-gluon system, which reads

$$(T_1^a + T_2^a + T_{1'}^a + T_{2'}^a)|R\overline{R}\rangle = 0. \quad (49)$$

As we work with states in which the dipole 1 2 and the conjugate dipole $1'2'$ are in definite color representations, we have

$$(T_1^a + T_2^a)^2|R\overline{R}\rangle = (T_{1'}^a + T_{2'}^a)^2|R\overline{R}\rangle = C_2[R]|R\overline{R}\rangle, \quad (50)$$

which we can use to simplify the cross product terms, e.g.

$$T_1^aT_2^a = T_{1'}^aT_{2'}^a = \tfrac{1}{2}(C_2[R] - 2C_A), \quad (51)$$

where we used that $T_j^aT_j^a = C_A$ for all j.[2] Now notice that for the operators

$$\begin{aligned} T_D^a &\equiv T_1^a + T_2^a = T^a \otimes 1 \otimes 1 \otimes 1 + 1 \otimes T^a \otimes 1 \otimes 1, \\ T_{D'}^a &\equiv T_{1'}^a + T_{2'}^a = 1 \otimes 1 \otimes T^a \otimes 1 + 1 \otimes 1 \otimes 1 \otimes T^a, \\ \Delta_D^a &\equiv T_1^a - T_2^a = T^a \otimes 1 \otimes 1 \otimes 1 - 1 \otimes T^a \otimes 1 \otimes 1, \\ \Delta_{D'}^a &\equiv T_{1'}^a - T_{2'}^a = 1 \otimes 1 \otimes T^a \otimes 1 - 1 \otimes 1 \otimes 1 \otimes T^a \end{aligned} \quad (52)$$

we have

$$T_D^a\Delta_D^a = (T_1^a)^2 - (T_2^a)^2 = 0 = T_{D'}^a\Delta_{D'}^a, \quad (53)$$

and, because of the color-singlet condition $T_D^a = -T_{D'}^a$, also

$$T_{D'}^a\Delta_D^a = T_D^a\Delta_{D'}^a = 0, \quad (54)$$

and, effectively

$$T_D^aT_{D'}^a = -T_D^aT_D^a = -C_2[R]. \quad (55)$$

Now insert

$$\begin{aligned} T_1^a &= \tfrac{1}{2}(T_D^a + \Delta_D^a); & T_2^a &= \tfrac{1}{2}(T_D^a - \Delta_D^a); \\ T_{1'}^a &= \tfrac{1}{2}(T_{D'}^a + \Delta_{D'}^a); & T_{2'}^a &= \tfrac{1}{2}(T_{D'}^a - \Delta_{D'}^a) \end{aligned} \quad (56)$$

into (48), and use relations (51) and (53)–(55) to obtain

$$\begin{aligned} 1 - \mathsf{S}_N^{(4)}(\boldsymbol{b}_1, \boldsymbol{b}_2, \boldsymbol{b}'_1, \boldsymbol{b}'_2) &= \tfrac{1}{2}C_A(\chi^2(\boldsymbol{b}_1) + \chi^2(\boldsymbol{b}_2) + \chi^2(\boldsymbol{b}'_1) + \chi^2(\boldsymbol{b}'_2)) + \tfrac{1}{2}(C_2[R] - 2C_A)(\chi(\boldsymbol{b}_1)\chi(\boldsymbol{b}_2) + \chi(\boldsymbol{b}'_1)\chi(\boldsymbol{b}'_2)) \\ &\quad - \tfrac{1}{4}C_2[R](\chi(\boldsymbol{b}'_1)\chi(\boldsymbol{b}_2) + \chi(\boldsymbol{b}_1)\chi(\boldsymbol{b}'_2) + \chi(\boldsymbol{b}_1)\chi(\boldsymbol{b}'_1) + \chi(\boldsymbol{b}_2)\chi(\boldsymbol{b}'_2)) \\ &\quad + \tfrac{1}{4}\Delta_D^a\Delta_{D'}^a(\chi(\boldsymbol{b}_1)\chi(\boldsymbol{b}'_1) + \chi(\boldsymbol{b}_2)\chi(\boldsymbol{b}'_2) - \chi(\boldsymbol{b}'_1)\chi(\boldsymbol{b}_2) - \chi(\boldsymbol{b}_1)\chi(\boldsymbol{b}'_2)). \end{aligned} \quad (57)$$

We can now go ahead and complete the squares,

$$\begin{aligned} 1 - \mathsf{S}_N^{(4)}(\boldsymbol{b}_1, \boldsymbol{b}_2, \boldsymbol{b}'_1, \boldsymbol{b}'_2) &= \tfrac{1}{4}(2C_A - C_2[R])[(\chi(\boldsymbol{b}_1) - \chi(\boldsymbol{b}_2))^2 + (\chi(\boldsymbol{b}'_1) - \chi(\boldsymbol{b}'_2))^2] + \tfrac{1}{8}C_2[R][(\chi(\boldsymbol{b}_1) - \chi(\boldsymbol{b}'_1))^2 \\ &\quad + (\chi(\boldsymbol{b}_2) - \chi(\boldsymbol{b}'_2))^2 + (\chi(\boldsymbol{b}'_1) - \chi(\boldsymbol{b}_2))^2 + (\chi(\boldsymbol{b}_1) - \chi(\boldsymbol{b}'_2))^2] + \tfrac{1}{8}\Delta_D^a\Delta_{D'}^a[(\chi(\boldsymbol{b}'_1) - \chi(\boldsymbol{b}_2))^2 \\ &\quad + (\chi(\boldsymbol{b}_1) - \chi(\boldsymbol{b}'_2))^2 - (\chi(\boldsymbol{b}_1) - \chi(\boldsymbol{b}'_1))^2 - (\chi(\boldsymbol{b}_2) - \chi(\boldsymbol{b}'_2))^2]. \end{aligned} \quad (58)$$

Finally, using (17) we obtain the following form for the dipole cross section operator for the four-gluon system

[2] Here a sum over a, but not j, is implied

$$\langle R'\overline{R'}|\hat{\sigma}^{(4)}(\boldsymbol{b}_1, \boldsymbol{b}_2, \boldsymbol{b}_1', \boldsymbol{b}_2')|R\overline{R}\rangle = \lambda_R \delta_{R',R} \cdot [\sigma(\boldsymbol{b}_1 - \boldsymbol{b}_2) + \sigma(\boldsymbol{b}_1' - \boldsymbol{b}_2')] + \frac{(1-\lambda_R)}{2}\delta_{R',R} \cdot [\sigma(\boldsymbol{b}_1 - \boldsymbol{b}_1') + \sigma(\boldsymbol{b}_2 - \boldsymbol{b}_2') + \sigma(\boldsymbol{b}_1' - \boldsymbol{b}_2) + \sigma(\boldsymbol{b}_1 - \boldsymbol{b}_2')] - \frac{\langle R'\overline{R'}|\Delta_D^a \Delta_{D'}^a|R\overline{R}\rangle}{4C_A} \cdot \Omega(\boldsymbol{b}_1, \boldsymbol{b}_2, \boldsymbol{b}_1', \boldsymbol{b}_2'). \quad (59)$$

Here the parameter

$$\lambda_R = 1 - \frac{C_2[R]}{2C_A}, \quad (60)$$

enters the diagonal part of the cross section and can be found for individual multiplets in Table I. In the off-diagonal piece we introduced the combination

$$\begin{aligned}\Omega(\boldsymbol{b}_1, \boldsymbol{b}_2, \boldsymbol{b}_1', \boldsymbol{b}_2') &\equiv \sigma(\boldsymbol{b}_1' - \boldsymbol{b}_2) + \sigma(\boldsymbol{b}_1 - \boldsymbol{b}_1') \\ &\quad - \sigma(\boldsymbol{b}_1 - \boldsymbol{b}_1') - \sigma(\boldsymbol{b}_2 - \boldsymbol{b}_2') \\ &= \sigma(\boldsymbol{s} + \boldsymbol{r}) + \sigma(\boldsymbol{s} - \boldsymbol{r}') - \sigma(\boldsymbol{s}) \\ &\quad - \sigma(\boldsymbol{s} + \boldsymbol{r} - \boldsymbol{r}'), \end{aligned} \quad (61)$$

the same structure of dipole cross sections made already an appearance in our previous solutions of the $q\bar{q}q\bar{q}$ and $qg\bar{q}g$ dipole cross section matrices [2,6]. Equation (59) is the central result of this subsection. We now turn to the evaluation of the matrix elements $\langle R'\overline{R'}|\Delta_D^a \Delta_{D'}^a|R\overline{R}\rangle$.

D. Evaluation of the off-diagonal matrix elements

For $R \neq R'$, we have

$$\langle R'\overline{R'}|\hat{\sigma}^{(4)}(\boldsymbol{b}_1, \boldsymbol{b}_2, \boldsymbol{b}_1', \boldsymbol{b}_2')|R\overline{R}\rangle = -\frac{\langle R'\overline{R'}|\Delta_D^a \Delta_{D'}^a|R\overline{R}\rangle}{4C_A} \times \Omega(\boldsymbol{b}_1, \boldsymbol{b}_2, \boldsymbol{b}_1', \boldsymbol{b}_2'). \quad (62)$$

We recall that

$$\begin{aligned}\Delta_D^a \Delta_{D'}^a &= (T^a \otimes 1 - 1 \otimes T^a) \otimes (T^a \otimes 1 - 1 \otimes T^a) \\ &= T^a \otimes 1 \otimes T^a \otimes 1 - 1 \otimes T^a \otimes T^a \otimes 1 \\ &\quad - T^a \otimes 1 \otimes 1 \otimes T^a + 1 \otimes T^a \otimes 1 \otimes T^a. \end{aligned} \quad (63)$$

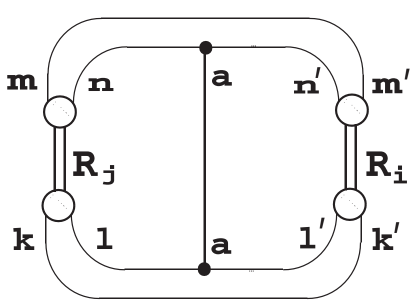

FIG. 6. The matrix element $\langle R_j\overline{R_j}|\hat{\mathcal{O}}|R_i\overline{R_i}\rangle$.

One can easily convince oneself that this is really a transition operator, i.e., it has only matrix elements between different multiplets, and even more they must be of different permutation symmetry, i.e. the transitions are between symmetric and antisymmetric multiplets. One can then use permutation symmetry, to obtain, effectively,

$$\begin{aligned}\Delta_D^a \Delta_{D'}^a &= 4 \cdot (1 \otimes T^a \otimes 1 \otimes T^a) \\ &= -4 \cdot (1 \otimes T^a \otimes 1 \otimes (T^a)^t) \equiv 4 \cdot \hat{\mathcal{O}}, \end{aligned} \quad (64)$$

which means

$$\langle R'\overline{R'}|\hat{\sigma}^{(4)}(\boldsymbol{b}_1, \boldsymbol{b}_2, \boldsymbol{b}_1', \boldsymbol{b}_2')|R\overline{R}\rangle = -\frac{1}{N_c} \cdot \langle R'\overline{R'}|\hat{\mathcal{O}}|R\overline{R}\rangle \cdot \Omega(\boldsymbol{b}_1, \boldsymbol{b}_2, \boldsymbol{b}_1', \boldsymbol{b}_2'). \quad (65)$$

Between four-gluon states with color wave functions A_{jk}^{mn}, B_{jk}^{mn} the matrix element of the operator $\hat{\mathcal{O}}$ is evaluated explicitly as

$$\langle A|\hat{\mathcal{O}}|B\rangle = A_{kl}^{mn} if_{nan'} if_{all'} \delta_{mm'} \delta_{kk'} B_{m'n'}^{k'l'}. \quad (66)$$

See also Fig. 6.

In Table II we collect the contractions of the operator $\hat{O}$ between a convenient choice of tensors, from which the matrix elements of the relevant four-gluon states (46) can be reconstructed. The tensor iY decouples completely—all its off-diagonal elements vanish.

E. The dipole cross section operator for the four-gluon system

We now come to the final result for the four-body dipole cross section operator in the s-channel basis described in Sec. IV B above, in which the two gluons from the amplitude and from the complex conjugate amplitude, respectively, are in definite color multiplets.

1. Diagonal elements

The diagonal elements for the four-gluon system are even simpler than for the quark-antiquark–gluon-gluon system studied in [6] and are expressed in terms of two combinations of color-dipole cross sections:

TABLE II. Matrix elements of the operator $\hat{\mathcal{O}}$.

	S	$P[1]$	$P[8_S]$	D_u	D_t
$\mathcal{A}$	$\frac{1}{4}N_c(N_c^2-1)^2$	N_c	$\frac{3}{4}N_c(N_c^2-1)$	$\frac{1}{2}(N_c^2-1)(N_c^2-4)$	$-\frac{1}{4}(N_c^2-1)(N_c^2-4)$
$P[8_A]$	$\frac{3}{4}N_c(N_c^2-1)$	N_c	$\frac{1}{4}N_c(N_c^2-1)$	0	$\frac{1}{4}(N_c^2-1)(N_c^2-4)$
iY	0	0	0	0	0

$$\begin{aligned}\Sigma_1 &\equiv \sigma(\boldsymbol{b}_1-\boldsymbol{b}_2)+\sigma(\boldsymbol{b}'_1-\boldsymbol{b}'_2)=\sigma(\boldsymbol{r})+\sigma(-\boldsymbol{r}'),\\ \tau &\equiv \sigma(\boldsymbol{b}_1-\boldsymbol{b}'_1)+\sigma(\boldsymbol{b}_2-\boldsymbol{b}'_2)+\sigma(\boldsymbol{b}'_1-\boldsymbol{b}_2)\\ &\quad+\sigma(\boldsymbol{b}_1-\boldsymbol{b}'_2)\\ &=\sigma(\boldsymbol{s}+\boldsymbol{r})+\sigma(\boldsymbol{s}-\boldsymbol{r}')+\sigma(\boldsymbol{s})+\sigma(\boldsymbol{s}+\boldsymbol{r}-\boldsymbol{r}'). \end{aligned} \tag{67}$$

Making use of Table I, we find

$$\begin{aligned}\langle 11|\hat{\sigma}^{(4)}|11\rangle &= \Sigma_{1,}\\ \langle 8_A8_A|\hat{\sigma}^{(4)}|8_A8_A\rangle &= \langle 8_S8_S|\hat{\sigma}^{(4)}|8_S8_S\rangle = \frac{1}{4}\tau+\frac{1}{2}\Sigma_1,\\ \langle 10\overline{10}|\hat{\sigma}^{(4)}|10\overline{10}\rangle &= \langle \overline{10}10|\hat{\sigma}^{(4)}|\overline{10}10\rangle = \frac{1}{2}\tau\\ &= \frac{C_2[10]}{C_A}\cdot\frac{1}{4}\tau,\\ \langle 2727|\hat{\sigma}^{(4)}|2727\rangle &= \frac{2(N_c+1)}{N_c}\cdot\frac{1}{4}\tau-\frac{1}{2N_c}\Sigma_1\\ &= \frac{C_2[27]}{C_A}\cdot\frac{1}{4}\tau-\frac{1}{2N_c}\Sigma_1,\\ \langle R_7R_7|\hat{\sigma}^{(4)}|R_7R_7\rangle &= \frac{2(N_c-1)}{N_c}\cdot\frac{1}{4}\tau+\frac{1}{2N_c}\Sigma_1\\ &= \frac{C_2[R_7]}{C_A}\cdot\frac{1}{4}\tau+\frac{1}{2N_c}\Sigma_1. \end{aligned} \tag{68}$$

We recall that in the limit of $\boldsymbol{r}=\boldsymbol{r}'=0$ the gluon pairs collapse into pointlike partons in the color-representation R_i. In this limit $\Sigma_1=0$, and the diagonal matrix elements are simply proportional to the Casimir operators as it must be [6]:

$$\langle R_iR_i|\hat{\sigma}^{(4)}|R_iR_i\rangle = \frac{C_2[R_i]}{C_A}\sigma(\boldsymbol{s}). \tag{69}$$

Notice that the matrix elements $\langle 2727|\hat{\sigma}^{(4)}|2727\rangle$ and $\langle R_7R_7|\hat{\sigma}^{(4)}|R_7R_7\rangle$ are related by the transformation $N_c\to -N_c$; for the discussion of a similar symmetry in the quark-gluon dijet production see Ref. [6].

2. Off-diagonal elements

Making use of Tables I and II we have

$$\begin{aligned}\langle 11|\hat{\sigma}^{(4)}|8_A8_A\rangle &= -\frac{1}{\sqrt{N_c^2-1}}\cdot\Omega(\boldsymbol{b}_1,\boldsymbol{b}_2,\boldsymbol{b}'_1,\boldsymbol{b}'_2),\\ \langle 8_S8_S|\hat{\sigma}^{(4)}|8_A8_A\rangle &= -\frac{1}{4}\cdot\Omega(\boldsymbol{b}_1,\boldsymbol{b}_2,\boldsymbol{b}'_1,\boldsymbol{b}'_2),\\ \langle 2727|\hat{\sigma}^{(4)}|8_A8_A\rangle &= -\frac{1}{2N_c}\sqrt{\frac{N_c+3}{N_c+1}}\cdot\Omega(\boldsymbol{b}_1,\boldsymbol{b}_2,\boldsymbol{b}'_1,\boldsymbol{b}'_2),\\ \langle R_7R_7|\hat{\sigma}^{(4)}|8_A8_A\rangle &= -\frac{1}{2N_c}\sqrt{\frac{N_c-3}{N_c-1}}\cdot\Omega(\boldsymbol{b}_1,\boldsymbol{b}_2,\boldsymbol{b}'_1,\boldsymbol{b}'_2),\\ \langle 8_S8_S|\hat{\sigma}^{(4)}|10\overline{10}\rangle &= -\frac{1}{2\sqrt{N_c^2-4}}\cdot\Omega(\boldsymbol{b}_1,\boldsymbol{b}_2,\boldsymbol{b}'_1,\boldsymbol{b}'_2)\\ &= \langle 8_S8_S|\hat{\sigma}^{(4)}|\overline{10}10\rangle,\\ \langle 2727|\hat{\sigma}^{(4)}|10\overline{10}\rangle &= -\frac{1}{4N_c}\sqrt{\frac{(N_c+1)(N_c-2)(N_c+3)}{N_c+2}}\\ &\quad\cdot\Omega(\boldsymbol{b}_1,\boldsymbol{b}_2,\boldsymbol{b}'_1,\boldsymbol{b}'_2)\\ &= \langle 2727|\hat{\sigma}^{(4)}|\overline{10}10\rangle,\\ \langle R_7R_7|\hat{\sigma}^{(4)}|10\overline{10}\rangle &= -\frac{1}{4N_c}\sqrt{\frac{(N_c-1)(N_c+2)(N_c-3)}{N_c-2}}\\ &\quad\cdot\Omega(\boldsymbol{b}_1,\boldsymbol{b}_2,\boldsymbol{b}'_1,\boldsymbol{b}'_2)\\ &= \langle R_7R_7|\hat{\sigma}^{(4)}|\overline{10}10\rangle. \end{aligned} \tag{70}$$

We again observe the curious symmetry [6]: the matrix elements $\langle 2727|\hat{\sigma}^{(4)}|8_A8_A\rangle$ and $\langle R_7R_7|\hat{\sigma}^{(4)}|8_A8_A\rangle$ are related by the transformation $N_c\to -N_c$; the same is true of the matrix elements $\langle 2727|\hat{\sigma}^{(4)}|\overline{10}10\rangle$ and $\langle R_7R_7|\hat{\sigma}^{(4)}|10\overline{10}\rangle$.

F. Large-N_c properties of the dipole cross section matrix

In conjunction with the Glauber-Gribov form for the nuclear S matrix, the dipole cross section operator $\hat{\sigma}^{(4)}$ solves the problem of non-Abelian intranuclear evolution of the four-gluon system. Being a symmetric matrix, the dipole cross section operator could readily be brought in diagonal form, and the Fourier transform could finally be performed numerically. In practice, however one would encounter a number of obstacles when proceeding along these lines. First, for the case of the two-particle inclusive spectrum, the eigenvalues of the dipole cross section operator will be nonanalytic functionals of the free-nucleon cross section operator, and second the dipole cross section itself has a nonanalytic dependence on dipole size, which would ultimately determine the asymptotics of the relevant Fourier transforms. It is therefore convenient that the large-N_c expansion offers a path to analytic formulas, which can be interpreted in a transparent way.

We start from the observation that at large-N_c the cross section operator $\hat{\sigma}^{(4)}$ assumes a block diagonal form. Apparently, transitions between representations which have dimensions that grow with the same power of N_c are parametrically of order N_c^0, whereas transitions to the next-larger/smaller block are suppressed by N_c^{-1}.

In the space of four-parton states we introduce the projectors

$$\begin{aligned} \mathcal{P}_1 &= |11\rangle\langle 11|, \\ \mathcal{P}_2 &= |8_A 8_A\rangle\langle 8_A 8_A| + |8_S 8_S\rangle\langle 8_S 8_S|, \\ \mathcal{P}_3 &= |10\overline{10}\rangle\langle 10\overline{10}| + |\overline{10}10\rangle\langle\overline{10}10| \\ &\quad + |2727\rangle\langle 2727| + |R_7 R_7\rangle\langle R_7 R_7|, \end{aligned} \tag{71}$$

which allow us to isolate the blocks $\mathcal{P}_i \hat{\sigma}^{(4)} \mathcal{P}_i$, the first one being a one-by-one matrix:

$$\mathcal{P}_1 \hat{\sigma}^{(4)} \mathcal{P}_1 = \Sigma_1. \tag{72}$$

The vector $|e_1\rangle = |11\rangle$ can be viewed as an eigenvector of block 1 with eigen cross section Σ_1.

The second block is written, in the two-dimensional subspace of octets, as

$$\mathcal{P}_2 \hat{\sigma}^{(4)} \mathcal{P}_2 = \begin{pmatrix} \frac{1}{4}[\tau + 2\Sigma_1] & -\frac{1}{4}\Omega \\ -\frac{1}{4}\Omega & \frac{1}{4}[\tau + 2\Sigma_1] \end{pmatrix}. \tag{73}$$

Its eigenvectors are

$$\begin{aligned} |e_2\rangle &= \frac{1}{\sqrt{2}}(|8_A 8_A\rangle + |8_S 8_S\rangle), \\ |e_3\rangle &= \frac{1}{\sqrt{2}}(|8_A 8_A\rangle - |8_S 8_S\rangle), \end{aligned} \tag{74}$$

and belong to the eigen cross sections

$$\begin{aligned} \Sigma_2 &= \tfrac{1}{2}\Sigma_1 + \tfrac{1}{4}[\tau - \Omega] \\ &= \tfrac{1}{2}(\Sigma_1 + \sigma(\boldsymbol{b}_1 - \boldsymbol{b}_1') + \sigma(\boldsymbol{b}_2 - \boldsymbol{b}_2')) \\ &= \tfrac{1}{2}[\sigma(\boldsymbol{r}) + \sigma(-\boldsymbol{r}') + \sigma(\boldsymbol{s}) + \sigma(\boldsymbol{s} + \boldsymbol{r} - \boldsymbol{r}')], \\ \Sigma_3 &= \tfrac{1}{2}\Sigma_1 + \tfrac{1}{4}[\tau + \Omega] \\ &= \tfrac{1}{2}[\Sigma_1 + \sigma(\boldsymbol{b}_1' - \boldsymbol{b}_2) + \sigma(\boldsymbol{b}_1 - \boldsymbol{b}_2')] \\ &= \tfrac{1}{2}[\sigma(\boldsymbol{r}) + \sigma(-\boldsymbol{r}') + \sigma(\boldsymbol{s} + \boldsymbol{r}) + \sigma(\boldsymbol{s} - \boldsymbol{r}')]. \end{aligned} \tag{75}$$

Finally, the third block accounts for the multiplets that have $\mathcal{O}(N_c^4)$ states. Here we notice that at large N_c all higher multiplets interact as two color-uncorrelated gluons. For instance, the Casimir operators for these multiplets approach $C_2(R_i) = 2C_A$ and the diagonal cross sections become identical. In matrix form, where the rows refer to states $|10\overline{10}\rangle$, $|\overline{10}10\rangle$, $|2727\rangle$, $|R_7R_7\rangle$ we write

$$\mathcal{P}_3 \hat{\sigma}^{(4)} \mathcal{P}_3 = \begin{pmatrix} \frac{1}{2}\tau & 0 & -\frac{1}{4}\Omega & -\frac{1}{4}\Omega \\ 0 & \frac{1}{2}\tau & -\frac{1}{4}\Omega & -\frac{1}{4}\Omega \\ -\frac{1}{4}\Omega & -\frac{1}{4}\Omega & \frac{1}{2}\tau & 0 \\ -\frac{1}{4}\Omega & -\frac{1}{4}\Omega & 0 & \frac{1}{2}\tau \end{pmatrix}. \tag{76}$$

Its eigenvectors are seen easily to be

$$\begin{aligned} |e_4\rangle &= \tfrac{1}{2}(|10\overline{10}\rangle + |\overline{10}10\rangle + |2727\rangle + |R_7R_7\rangle), \\ |e_5\rangle &= \tfrac{1}{2}(|10\overline{10}\rangle + |\overline{10}10\rangle - |2727\rangle - |R_7R_7\rangle), \\ |e_6\rangle &= \frac{1}{\sqrt{2}}(|10\overline{10}\rangle - |\overline{10}10\rangle), \\ |e_7\rangle &= \frac{1}{\sqrt{2}}(|2727\rangle - |R_7R_7\rangle), \end{aligned} \tag{77}$$

with eigenvalues

$$\begin{aligned} \Sigma_4 &= \tfrac{1}{2}(\tau - \Omega) = \sigma(\boldsymbol{b}_1 - \boldsymbol{b}_1') + \sigma(\boldsymbol{b}_2 - \boldsymbol{b}_2') \\ &= \sigma(\boldsymbol{s}) + \sigma(\boldsymbol{s} + \boldsymbol{r} - \boldsymbol{r}'), \\ \Sigma_5 &= \tfrac{1}{2}(\tau + \Omega) = \sigma(\boldsymbol{b}_1' - \boldsymbol{b}_2) + \sigma(\boldsymbol{b}_1 - \boldsymbol{b}_2') \\ &= \sigma(\boldsymbol{s} + \boldsymbol{r}) + \sigma(\boldsymbol{s} - \boldsymbol{r}'), \\ \Sigma_6 &= \Sigma_7 = \tfrac{1}{2}\tau = \tfrac{1}{2}(\Sigma_4 + \Sigma_5). \end{aligned} \tag{78}$$

We finally observe that the eigenstate $|e_6\rangle$ decouples exactly from our problem, which is seen readily from the summary of the off-diagonal elements (70). Couplings between the above diagonalized matrix blocks are of $\mathcal{O}(N_c^{-1})$. In the basis of eigenstates $|e_1\rangle, \ldots, |e_7\rangle$ we can collect the N_c-suppressed off-diagonal elements as

$$\begin{aligned} \hat{\omega}(\boldsymbol{s}, \boldsymbol{r}, \boldsymbol{r}') = -\frac{1}{\sqrt{2}N_c}\Omega(\boldsymbol{s}, \boldsymbol{r}, \boldsymbol{r}')\{&|e_1\rangle\langle e_2| + |e_1\rangle\langle e_3| \\ &+ |e_4\rangle\langle e_2| - |e_5\rangle\langle e_3| + \text{H.c.}\}. \end{aligned} \tag{79}$$

It is easy to check that the off-diagonal elements containing the state $|e_7\rangle$ are $\mathcal{O}(N_c^{-2})$ and this state decouples at $\mathcal{O}(N_c^{-1})$. At $\mathcal{O}(N_c^{-1})$ there are also corrections to the diagonal matrix elements, in the sector of large symmetric representations $27, R_7$. They are however not relevant for our problem; the N_c^{-1} perturbation theory treatment of such corrections is found in [2]. The crucial observation is that in the inclusive dijet spectrum, with summation over all colors of final-state gluons, the final-state projection simplifies to

$$\begin{aligned} \sum_X \langle X| &= \sum_R \sqrt{\dim[R]}\langle R\bar{R}| \\ &= \underbrace{\langle e_1|}_{1} + \underbrace{N_c\sqrt{2}\langle e_2|}_{8_A + 8_S} + \underbrace{N_c^2\langle e_4|}_{10+\overline{10}+27+R_7}. \end{aligned} \tag{80}$$

If we remember that averaging over incoming colors shall introduce another factor $1/N_c$,

$$|\mathrm{in}\rangle = \frac{1}{\sqrt{\dim[8]}}|8_A 8_A\rangle = \frac{1}{\sqrt{2}N_c}(|e_2\rangle + |e_3\rangle), \tag{81}$$

we see that the large number of states in higher multiplets can overcome the suppression of their excitation. The excitation of singlet states is large-N_c suppressed and will be dealt with separately.

To develop the large-N_c perturbation theory, we decompose the free-nucleon cross section operator as

$$\hat{\sigma}^{(4)} = \hat{\Sigma}^{(0)} + \hat{\omega}, \tag{82}$$

where

$$\hat{\Sigma}^{(0)} = \mathcal{P}_1\hat{\sigma}^{(4)}\mathcal{P}_1 + \mathcal{P}_2\hat{\sigma}^{(4)}\mathcal{P}_2 + \mathcal{P}_3\hat{\sigma}^{(4)}\mathcal{P}_3 = \sum_{j=1}^{7}\Sigma_j|e_j\rangle\langle e_j| \tag{83}$$

is the block matrix that is diagonalized by the basis $|e_1\rangle \dots |e_7\rangle$. Now, the nuclear S matrix is obtained from the free-nucleon dipole cross section by means of the Glauber-Gribov exponentiation

$$\mathsf{S}[\boldsymbol{b}, \hat{\sigma}^{(4)}(\boldsymbol{s}, \boldsymbol{r}, \boldsymbol{r}')] = \exp[-\tfrac{1}{2}\hat{\sigma}^{(4)}(\boldsymbol{s}, \boldsymbol{r}, \boldsymbol{r}')T(\boldsymbol{b})]. \tag{84}$$

To the first order in the off-diagonal perturbation $\hat{\omega}$ we can establish easily

$$\mathsf{S}[\boldsymbol{b}, \hat{\Sigma}^{(0)} + \hat{\omega}] - \mathsf{S}[\boldsymbol{b}, \hat{\Sigma}^{(0)}] = -\frac{1}{2}T(\boldsymbol{b})\int_0^1 d\beta \mathsf{S}[\boldsymbol{b}, (1-\beta)\hat{\Sigma}^{(0)}]\hat{\omega}\mathsf{S}[\boldsymbol{b}, \beta\hat{\Sigma}^{(0)}] + \mathcal{O}(N_c^{-2}). \tag{85}$$

V. LINEAR $k_\perp$ FACTORIZATION FOR DIJETS FROM THE FREE-NUCLEON TARGET

At this point we are in a position to give our result for the process $g^* g_N \to g_1 g_2$ on the free-nucleon target. After integrating over the overall impact parameter, our master formula assumes the form

$$\frac{d\sigma_N(g^* \to g_1 g_2)}{dz d^2\boldsymbol{p}_1 d^2\boldsymbol{p}_2} = \frac{1}{2(2\pi)^4}\int d^2\boldsymbol{s} d^2\boldsymbol{r} d^2\boldsymbol{r}' \exp[-i\boldsymbol{\Delta s} - i\boldsymbol{p}_1(\boldsymbol{r} - \boldsymbol{r}')]\Psi(z, \boldsymbol{r})\Psi^*(z, \boldsymbol{r}')\sum_X \langle X|\hat{\Sigma}(\boldsymbol{s}, \boldsymbol{r}, \boldsymbol{r}')|in\rangle. \tag{86}$$

We evaluate the cross section for an incoming gluon, which entails an average over its incoming colors and the initial state $|in\rangle$ of Eq. (45). Likewise in the final state we sum over all color states. Then, the calculation of the inclusive cross section involves the evaluation of the following matrix elements of the four-parton cross section operator

$$\begin{aligned}\sum_{R\neq 8_A}\sqrt{\frac{\dim[R]}{\dim[8]}}\langle R\bar{R}|\hat{\Sigma}(\boldsymbol{s}, \boldsymbol{r}, \boldsymbol{r}')|8_A 8_A\rangle &= -\sum_{R\neq 8_A}\sqrt{\frac{\dim[R]}{N_c^2-1}}\langle R\bar{R}|\hat{\sigma}^{(4)}(\boldsymbol{s}, \boldsymbol{r}, \boldsymbol{r}')|8_A 8_A\rangle \\ &= \Omega(\boldsymbol{s}, \boldsymbol{r}, \boldsymbol{r}')\Bigg(\underbrace{\frac{1}{4}}_{8_S} + \underbrace{\frac{1}{N_c^2-1}}_{1} + \underbrace{\sqrt{\frac{N_c^2(N_c+3)(N_c-1)}{4(N_c^2-1)}}\frac{1}{2N_c}\sqrt{\frac{N_c+3}{N_c+1}}}_{27} \\ &\quad + \underbrace{\sqrt{\frac{N_c^2(N_c-3)(N_c+1)}{4(N_c^2-1)}}\frac{1}{2N_c}\sqrt{\frac{N_c-3}{N_c-1}}}_{R_7}\Bigg) \\ &= \frac{1}{4}\Omega(\boldsymbol{s}, \boldsymbol{r}, \boldsymbol{r}')\Bigg(\underbrace{1}_{8_S} + \underbrace{\frac{4}{N_c^2-1}}_{1} + \underbrace{\frac{N_c+3}{N_c+1}}_{27} + \underbrace{\frac{N_c-3}{N_c-1}}_{R_7}\Bigg) \\ &= \frac{1}{4}\Omega(\boldsymbol{s}, \boldsymbol{r}, \boldsymbol{r}')(\underbrace{1}_{8_S} + \underbrace{2}_{1+27+R_7}).\end{aligned} \tag{87}$$

Here we indicated the contributions from excitation of individual multiplets different from the antisymmetric octet representation of the incident gluon. $\Omega(\boldsymbol{s}, \boldsymbol{r}, \boldsymbol{r}')$ is the same as in Eq. (61); now in the relevant coordinates, explicitly

$$\Omega(\boldsymbol{s}, \boldsymbol{r}, \boldsymbol{r}') = \int d^2\boldsymbol{\kappa} f(\boldsymbol{\kappa}) \exp[i\boldsymbol{\kappa}\boldsymbol{s}](1 - \exp[i\boldsymbol{\kappa}\boldsymbol{r}])(1 - \exp[-i\boldsymbol{\kappa}\boldsymbol{r}']). \tag{88}$$

The diagonal contribution from final-state gluons in the antisymmetric octet is constructed easily from the results of Sec. IV:

$$\begin{aligned}\langle 8_A 8_A|\hat{\Sigma}(\boldsymbol{s}, \boldsymbol{r}, \boldsymbol{r}')|8_A 8_A\rangle &= \sigma^{(3)}(\boldsymbol{b}_1, \boldsymbol{b}_2, \boldsymbol{b}') + \sigma^{(3)}(\boldsymbol{b}_1', \boldsymbol{b}_2', \boldsymbol{b}) - \sigma(\boldsymbol{s} + z(\boldsymbol{r} - \boldsymbol{r}')) - \langle 8_A 8_A|\hat{\sigma}^{(4)}(\boldsymbol{s}, \boldsymbol{r}, \boldsymbol{r}')|8_A 8_A\rangle \\ &= \frac{1}{2}[\sigma(\boldsymbol{s} - z\boldsymbol{r}' + \boldsymbol{r}) + \sigma(\boldsymbol{s} - \boldsymbol{r}' + z\boldsymbol{r}) - \sigma(\boldsymbol{s} + z(\boldsymbol{r} - \boldsymbol{r}')) - \sigma(\boldsymbol{s} + \boldsymbol{r} - \boldsymbol{r}') + \sigma(\boldsymbol{s} - z\boldsymbol{r}') \\ &\quad + \sigma(\boldsymbol{s} + z\boldsymbol{r}) - \sigma(\boldsymbol{s} + z(\boldsymbol{r} - \boldsymbol{r}')) - \sigma(\boldsymbol{s})] - \frac{1}{4}[\sigma(\boldsymbol{s} - \boldsymbol{r}') + \sigma(\boldsymbol{s} + \boldsymbol{r}) - \sigma(\boldsymbol{s} + \boldsymbol{r} - \boldsymbol{r}') - \sigma(\boldsymbol{s})] \\ &= \int d^2\boldsymbol{\kappa} f(\boldsymbol{\kappa}) \exp[i\boldsymbol{\kappa}\boldsymbol{s}]\bigg\{\frac{1}{2}(\exp[i\boldsymbol{\kappa}\boldsymbol{r}] - \exp[iz\boldsymbol{\kappa}\boldsymbol{r}])(\exp[-i\boldsymbol{\kappa}\boldsymbol{r}'] - \exp[-iz\boldsymbol{\kappa}\boldsymbol{r}']) \\ &\quad + \frac{1}{2}(1 - \exp[iz\boldsymbol{\kappa}\boldsymbol{r}])(1 - \exp[-iz\boldsymbol{\kappa}\boldsymbol{r}']) - \frac{1}{4}(1 - \exp[i\boldsymbol{\kappa}\boldsymbol{r}])(1 - \exp[-i\boldsymbol{\kappa}\boldsymbol{r}'])\bigg\}. \end{aligned} \tag{89}$$

The dijet cross section for production of gluons in the antisymmetric octet reads therefore

$$\begin{aligned}\frac{d\sigma_N(g^* \to \{g_1 g_2\}_{8_A})}{dz d^2\boldsymbol{\Delta} d^2\boldsymbol{p}} &= \frac{1}{2(2\pi)^2} f(\boldsymbol{\Delta}) \\ &\times \bigg\{|\Psi(z, \boldsymbol{p} - \boldsymbol{\Delta}) - \Psi(z, \boldsymbol{p} - z\boldsymbol{\Delta})|^2 \\ &+ |\Psi(z, \boldsymbol{p}) - \Psi(z, \boldsymbol{p} - z\boldsymbol{\Delta})|^2 \\ &- \frac{1}{2}|\Psi(z, \boldsymbol{p}) - \Psi(z, \boldsymbol{p} - \boldsymbol{\Delta})|^2\bigg\}, \end{aligned} \tag{90}$$

The wave function of the gluon-gluon Fock state of the physical gluon enters our analysis as the recurrent quantity

$$\begin{aligned}|\Psi(z, \boldsymbol{p}) - \Psi(z, \boldsymbol{p} - \boldsymbol{\kappa})|^2 &= 2\alpha_S P_{gg}(z) \\ &\times \left(\frac{\boldsymbol{p}}{\boldsymbol{p}^2 + \varepsilon^2} - \frac{\boldsymbol{p} - \boldsymbol{\kappa}}{(\boldsymbol{p} - \boldsymbol{\kappa})^2 + \varepsilon^2}\right)^2, \end{aligned} \tag{91}$$

where $P_{gg}(z)$ is the familiar gluon-splitting function,

$$\begin{aligned}P_{gg}(z) &= 2C_A\left[\frac{1 - z}{z} + \frac{z}{1 - z} + z(1 - z)\right], \\ \varepsilon^2 &= z(1 - z)(Q^*)^2. \end{aligned} \tag{92}$$

Now notice that the last contribution in (90) would be canceled exactly, in the fully inclusive sum, by the excitation of symmetric octets. Summing over all possible final states we end up with

$$\begin{aligned}\frac{d\sigma_N(g^* \to g_1 g_2)}{dz d^2\boldsymbol{\Delta} d^2\boldsymbol{p}} &= \frac{1}{2(2\pi)^2} f(\boldsymbol{\Delta}) \\ &\times \{|\Psi(z, \boldsymbol{p} - \boldsymbol{\Delta}) - \Psi(z, \boldsymbol{p} - z\boldsymbol{\Delta})|^2 \\ &+ |\Psi(z, \boldsymbol{p}) - \Psi(z, \boldsymbol{p} - z\boldsymbol{\Delta})|^2 \\ &+ |\Psi(z, \boldsymbol{p}) - \Psi(z, \boldsymbol{p} - \boldsymbol{\Delta})|^2\}, \end{aligned} \tag{93}$$

where now the last term sums up the contribution from excitation of $1, 27, R_7$, whereas the first two terms represent the sum of octet $8_A, 8_S$ final states. No large N_c approximation has been invoked here; what would change with N_c is only the composition of the final state, where the excitation of color-singlet states is $\mathcal{O}(N_c^{-2})$. The absence of decuplet excitation is a consequence of the excitation mechanism being single-gluon exchange. Our result Eq. (93) is of course nothing but the differential version of Eq. (82) of Ref. [4], further elucidating the color-composition of the final state. By itself it would find interesting phenomenological applications to dijet production in a regime where saturation/absorption effects are not strong, e.g. central dijets at HERA or semihard dijets at Tevatron.

VI. NONLINEAR $k_\perp$ FACTORIZATION FOR DIJETS FROM NUCLEAR TARGETS

A. Dijets in color-octet final states

In order to evaluate our master formula for the case of octet-final states we have to collect the various multiparton S matrices. The three- and two-body S matrices are single-channel problems and can be written in terms of the Glauber-Gribov exponential as

$$\begin{aligned} \mathsf{S}^{(3)}_{g_1' g_2' g^*} &= \mathsf{S}[\boldsymbol{b}, \sigma_{g_1' g_2' g^*}] \\ &= \mathsf{S}[\boldsymbol{b}, \tfrac{1}{2}\sigma(\boldsymbol{r})]\mathsf{S}[\boldsymbol{b}, \tfrac{1}{2}\sigma(\boldsymbol{s} - z\boldsymbol{r}' + \boldsymbol{r})] \\ &\quad \times \mathsf{S}[\boldsymbol{b}, \tfrac{1}{2}\sigma(\boldsymbol{s} - z\boldsymbol{r}')], \\ \mathsf{S}^{(3)}_{g_1 g_2 g'^*} &= \mathsf{S}[\boldsymbol{b}, \sigma_{g_1 g_2 g'^*}] \\ &= \mathsf{S}[\boldsymbol{b}, \tfrac{1}{2}\sigma(\boldsymbol{r}')]\mathsf{S}[\boldsymbol{b}, \tfrac{1}{2}\sigma(\boldsymbol{s} - \boldsymbol{r}' + z\boldsymbol{r})] \\ &\quad \times \mathsf{S}[\boldsymbol{b}, \tfrac{1}{2}\sigma(\boldsymbol{s} + z\boldsymbol{r})], \\ \mathsf{S}^{(2)}_{g^* g'^*} &= \mathsf{S}[\boldsymbol{b}, \sigma_{g^* g'^*}] = \mathsf{S}[\boldsymbol{b}, \sigma(\boldsymbol{s} + z(\boldsymbol{r} - \boldsymbol{r}'))] \\ &= \mathsf{S}^2[\boldsymbol{b}, \tfrac{1}{2}\sigma(\boldsymbol{s} + z(\boldsymbol{r} - \boldsymbol{r}'))]. \end{aligned} \tag{94}$$

Notice that the factorization of S matrices is an exact consequence of the form of the dipole cross section for the three-gluon state and of the Glauber-Gribov exponentiation valid for a large nucleus; it is not related to the large-N_c limit. We need to invoke the large-N_c approximation only for the contribution from the four-body S matrix

$$\begin{aligned}\langle e_2|\mathsf{S}[\boldsymbol{b},\hat{\Sigma}^{(0)}]|e_2\rangle &= \mathsf{S}[\boldsymbol{b},\Sigma_2]\\ &= \mathsf{S}[\boldsymbol{b},\tfrac{1}{2}\sigma(\boldsymbol{r})]\mathsf{S}[\boldsymbol{b},\tfrac{1}{2}\sigma(\boldsymbol{r}')]\mathsf{S}[\boldsymbol{b},\tfrac{1}{2}\sigma(\boldsymbol{s})]\\ &\quad\times S[\boldsymbol{b},\tfrac{1}{2}\sigma(\boldsymbol{s}+\boldsymbol{r}-\boldsymbol{r}')]. \end{aligned} \tag{95}$$

Our aim is to find a momentum-space representation in terms of the nuclear unintegrated glue. The latter is given by the pertinent function ϕ_g defined through [4]

$$1-\mathsf{S}[\boldsymbol{b},\tfrac{1}{2}\sigma(\boldsymbol{r})] \equiv \int d^2\boldsymbol{\kappa}\phi_g(\boldsymbol{b},\boldsymbol{\kappa})(1-\exp[i\boldsymbol{\kappa}\boldsymbol{r}]). \tag{96}$$

Notice a subtlety:

$$\begin{aligned}\mathsf{S}\left[\boldsymbol{b},\frac{1}{2}\sigma(\boldsymbol{r})\right] &= \exp\left[-\frac{1}{4}\sigma(\boldsymbol{r})T(\boldsymbol{b})\right]\\ &= \exp\left[-\frac{C_A}{4C_F}\sigma_{q\bar{q}}(\boldsymbol{r})T(\boldsymbol{b})\right],\end{aligned} \tag{97}$$

where we used the relationship between the dipole cross section $\sigma(\boldsymbol{r})$ defined for a gluon-gluon system and the quark-antiquark system,

$$\sigma(\boldsymbol{r}) = \frac{C_A}{C_F}\sigma_{q\bar{q}}(\boldsymbol{r}). \tag{98}$$

Consequently, the collective unintegrated nuclear glue $\phi_g(\boldsymbol{b},\boldsymbol{\kappa})$ is different form the nuclear unintegrated glue $\phi(\boldsymbol{b},\boldsymbol{\kappa})$ that enters deep inelastic scattering as well as diffractive quark-antiquark jet production and has been introduced in [2,8]. It should not be mixed up with yet another quantity, the unintegrated glue defined through the color-singlet gluon-gluon probe, $\phi_{gg}(\boldsymbol{b},\boldsymbol{\kappa})$, which is defined through (for more discussion see Appendix D)

$$1-\mathsf{S}[\boldsymbol{b},\sigma(\boldsymbol{r})] \equiv \int d^2\boldsymbol{\kappa}\phi_{gg}(\boldsymbol{b},\boldsymbol{\kappa})(1-\exp[i\boldsymbol{\kappa}\boldsymbol{r}]). \tag{99}$$

If we denote by

$$\sigma_0 \equiv \frac{C_A}{C_F}\int d^2\boldsymbol{\kappa}f(\boldsymbol{\kappa}) \tag{100}$$

the dipole cross section for a large gluon-gluon dipole, then ϕ_{gg}, ϕ_g are related by the momentum-space convolution,

$$\begin{aligned}\phi_{gg}(\boldsymbol{b},\boldsymbol{\kappa}) &= 2\mathsf{S}[\boldsymbol{b},\tfrac{1}{2}\sigma_0]\phi_g(\boldsymbol{b},\boldsymbol{\kappa}) + (\phi_g\otimes\phi_g)(\boldsymbol{b},\boldsymbol{\kappa}),\\ (\phi_g\otimes\phi_g)(\boldsymbol{b},\boldsymbol{\kappa}) &= \int d^2\boldsymbol{q}\phi_g(\boldsymbol{b},\boldsymbol{\kappa}-\boldsymbol{q})\phi_g(\boldsymbol{b},\boldsymbol{q}).\end{aligned} \tag{101}$$

Another useful quantity is

$$\Phi_g(\boldsymbol{b},\boldsymbol{\kappa}) = \mathsf{S}[\boldsymbol{b},\tfrac{1}{2}\sigma_0]\delta^{(2)}(\boldsymbol{\kappa}) + \phi_g(\boldsymbol{b},\boldsymbol{\kappa}), \tag{102}$$

in terms of which,

$$\mathsf{S}[\boldsymbol{b},\tfrac{1}{2}\sigma(\boldsymbol{r})] = \int d^2\boldsymbol{\kappa}\Phi_g(\boldsymbol{b},\boldsymbol{\kappa})\exp[i\boldsymbol{\kappa}\boldsymbol{r}]. \tag{103}$$

For later applications we shall also use the collective glue for a slice $0<\beta<1$ of a nucleus

$$\mathsf{S}[\boldsymbol{b},\tfrac{1}{2}\beta\sigma(\boldsymbol{r})] = \int d^2\boldsymbol{\kappa}\Phi_g(\beta;\boldsymbol{b},\boldsymbol{\kappa})\exp[i\boldsymbol{\kappa}\boldsymbol{r}]. \tag{104}$$

It has the convolution property $(\Phi_g(\beta_1)\otimes\Phi_g(\beta_2))\times(\boldsymbol{b},\boldsymbol{\kappa}) = \Phi_g(\beta_1+\beta_2;\boldsymbol{b},\boldsymbol{\kappa})$ and we note that Eq. (101) amounts to $\Phi_{gg}(\boldsymbol{b},\boldsymbol{\kappa}) = \Phi_g(2,\boldsymbol{b},\boldsymbol{\kappa})$.

Intranuclear attenuation of dipoles becomes manifest in the distorted wave functions, defined in dipole and momentum space, respectively, as

$$\begin{aligned}\Psi(\beta;z,\boldsymbol{r}) &\equiv \mathsf{S}[\boldsymbol{b},\tfrac{1}{2}\beta\sigma(\boldsymbol{r})]\Psi(z,\boldsymbol{r}),\\ \Psi(\beta;z,\boldsymbol{p}) &= \int d^2\boldsymbol{r}\exp[-i\boldsymbol{p}\boldsymbol{r}]\Psi(\beta;z,\boldsymbol{r})\\ &= \int d^2\boldsymbol{\kappa}\Phi_g(\boldsymbol{b},\boldsymbol{\kappa})\Psi(z,\boldsymbol{p}-\boldsymbol{\kappa}).\end{aligned} \tag{105}$$

Now, using our master formula, the inclusive dijet cross section for gluons in the octet final state unfolds as

$$\begin{aligned}\frac{d\sigma(g^*\to\{g_1g_2\}_{8_A+8_S})}{d^2\boldsymbol{b}dzd^2\boldsymbol{p}d^2} &= \frac{1}{(2\pi)^4}\int d^2\boldsymbol{s}d^2\boldsymbol{r}d^2\boldsymbol{r}'\exp[-i\boldsymbol{\Delta}\boldsymbol{s}]\exp[-i\boldsymbol{p}(\boldsymbol{r}-\boldsymbol{r}')]\bigg\{\Psi(1;z,\boldsymbol{r})\Psi^*(1;z,\boldsymbol{r}')\mathsf{S}\left[\boldsymbol{b},\frac{1}{2}\sigma(\boldsymbol{s}+\boldsymbol{r}-\boldsymbol{r}')\right]\\ &\quad\times\mathsf{S}\left[\boldsymbol{b},\frac{1}{2}\sigma(\boldsymbol{s})\right] + \Psi(z,\boldsymbol{r})\Psi^*(z,\boldsymbol{r})\mathsf{S}^2\left[\boldsymbol{b},\frac{1}{2}\sigma(\boldsymbol{s}+z(\boldsymbol{r}-\boldsymbol{r}'))\right]\\ &\quad-\Psi(1;z,\boldsymbol{r})\Psi^*(z,\boldsymbol{r}')\mathsf{S}\left[\boldsymbol{b},\frac{1}{2}\sigma(\boldsymbol{s}-z\boldsymbol{r}'+\boldsymbol{r})\right]\mathsf{S}\left[\boldsymbol{b},\frac{1}{2}\sigma(\boldsymbol{s}-z\boldsymbol{r}')\right]\\ &\quad-\Psi(z,\boldsymbol{r})\Psi^*(1;z,\boldsymbol{r})\mathsf{S}\left[\boldsymbol{b},\frac{1}{2}\sigma(\boldsymbol{s}-\boldsymbol{r}'+z\boldsymbol{r})\right]\mathsf{S}\left[\boldsymbol{b},\frac{1}{2}\sigma(\boldsymbol{s}+z\boldsymbol{r})\right]\bigg\}\\ &= \frac{1}{2(2\pi)^2}\int d^2\boldsymbol{\kappa}_1\int d^2\boldsymbol{\kappa}_2\delta^{(2)}(\boldsymbol{\Delta}-\boldsymbol{\kappa}_1-\boldsymbol{\kappa}_2)\Phi_g(\boldsymbol{b},\boldsymbol{\kappa}_2)\Phi_g(\boldsymbol{b},\boldsymbol{\kappa}_1)\{|\Psi(1;z,\boldsymbol{p}-\boldsymbol{\kappa}_1)\\ &\quad-\Psi(z,\boldsymbol{p}-z\boldsymbol{\kappa}_1-z\boldsymbol{\kappa}_2)|^2 + |\Psi(1;z,\boldsymbol{p}-\boldsymbol{\kappa}_2)-\Psi(z,\boldsymbol{p}-z\boldsymbol{\kappa}_1-z\boldsymbol{\kappa}_2)|^2\}.\end{aligned} \tag{106}$$

Here we presented the result in a manifestly $\boldsymbol{\kappa}_1 \leftrightarrow \boldsymbol{\kappa}_2$ symmetric form. It is a nonlinear—fourth order—functional of the collective nuclear unintegrated glue. The origin of nonlinearity is crystal clear from Eqs. (94), (95), and (103): (i) the dipole cross section for multiparton states is a (matrix) superposition of cross sections for elementary dipoles, (ii) the corresponding nuclear S matrices are (matrix) products of S matrices for elementary dipoles, (iii) by virtue of (103) the nuclear distortion of the corresponding matrix element of the two-body density matrix is a multiple convolution of the collective nuclear glue. All the above is an indispensable feature of pQCD processes in a nuclear environment; any application of the linear $k_\perp$ factorization to the evaluation of nuclear effects in the dijet production is entirely unwarranted. The same comment applies to dijets in all other color representations.

Equation (106) shows very clearly how the quadratic- and cubic-nonlinear contributions from the two-body and three-body dipole states and the quartic-nonlinear contribution from the four-body state conspire to produce a difference of the intranuclear coherently distorted and the in-vacuum wave functions of the gg Fock state. It is useful to look also at the transition to the impulse approximation (IA), in which (see Appendix D)

$$\Phi_g(\boldsymbol{b}, \boldsymbol{\kappa}_2)\Phi_g(\boldsymbol{b}, \boldsymbol{\kappa}_1) = \delta^{(2)}(\boldsymbol{\kappa}_2)\delta^{(2)}(\boldsymbol{\kappa}_1) + \tfrac{1}{2}T(\boldsymbol{b}) \times [\delta^{(2)}(\boldsymbol{\kappa}_2)f(\boldsymbol{\kappa}_1) + \delta^{(2)}(\boldsymbol{\kappa}_1)f(\boldsymbol{\kappa}_2)]. \tag{107}$$

The contribution from the term $\delta^{(2)}(\boldsymbol{\kappa}_2)\delta^{(2)}(\boldsymbol{\kappa}_1)$ to the nuclear cross section (106) vanishes, while the terms linear in $T(\boldsymbol{b})$ recover precisely the octet component of free-nucleon cross section (93) times $T(\boldsymbol{b})$.

The result (106) fully conforms with the concept of universality classes introduced in Refs. [5,6] and must be compared to the dijet spectra of other reactions in which the dijets are produced in the same color representation as the incident parton: excitation of color-octet quark-antiquark dijet or of open heavy flavor from gluons, $g \to \{Q\bar{Q}\}_8$, and excitation of color-triplet quark-gluon dijets from quarks, $q \to \{qg\}_3$. The incoherent distortion factor $\Phi_g(\boldsymbol{b}, \boldsymbol{\kappa}_1)\Phi_g(\boldsymbol{b}, \boldsymbol{\kappa}_2)$ in the integrand is the same as in another gluon induced reaction $g \to Q\bar{Q}$. It must be compared to the distortion factor $\Phi_g(\boldsymbol{b}, \boldsymbol{\Delta})$ in the case of $q \to \{qg\}_3$. Following [5,6] we note that (i) to the considered large-N_c approximation the above $\Phi_g(\boldsymbol{b}, \boldsymbol{\kappa})$ equals the nuclear collective glue $\Phi(\boldsymbol{b}, \boldsymbol{\kappa})$ defined via the quark-antiquark dipoles, (ii) the incident gluon behaves as a pair of color-uncorrelated quark and antiquark propagating at the same impact parameter, and (iii) $\Phi_g(\boldsymbol{b}, \boldsymbol{\kappa}_2)\Phi_g(\boldsymbol{b}, \boldsymbol{\kappa}_1)$ can be considered as a product of distortion factors of this uncorrelated quark-antiquark pair. As in the case of $q \to \{qg\}_3$, we can treat

$$\tfrac{1}{2}\{|\Psi(1; z, \boldsymbol{p} - \boldsymbol{\kappa}_1) - \Psi(z, \boldsymbol{p} - z\boldsymbol{\Delta})|^2 + |\Psi(1; z, \boldsymbol{p} - \boldsymbol{\kappa}_2) - \Psi(z, \boldsymbol{p} - z\boldsymbol{\Delta})|^2\},$$

which contains the collinear singularity of the $g \to gg$ splitting, as an intranuclear-distorted hard fragmentation function of the quasielastically scattered gluon. In close similarity to the excitation $q \to \{qg\}_3$, one of the wave functions which enters the fragmentation function is coherently distorted over the whole thickness of the nucleus. The only difference is that with the incident gluon, the argument of the coherently distorted wave function is $\boldsymbol{p} - \boldsymbol{\kappa}_i$ versus $\boldsymbol{p} - \boldsymbol{\Delta}$ in the case of the incident quark in $q \to \{qg\}_3$.

B. Coherent diffractive dijets and the rapidity gap survival

The coherent diffractive back-to-back dijets form a universality class of their own [5,6]. They can readily be isolated from the generic octet-final states upon the application of the expansion (102):

$$\frac{d\sigma_D(g^* \to \{g_1 g_2\}_{8_A})}{d^2\boldsymbol{b}dz d^2\boldsymbol{p} d^2\boldsymbol{\Delta}} = \frac{1}{(2\pi)^2}\mathsf{S}[\boldsymbol{b}, \sigma_0]\delta^{(2)}(\boldsymbol{\Delta}) \times |\Psi(1; z, \boldsymbol{p}) - \Psi(z, \boldsymbol{p})|^2. \tag{108}$$

The incident gluon has a net color charge, and in close similarity to diffractive excitation of color-triplet quark-gluon dijets from quarks, $q \to \{qg\}_3$, the coherent diffractive cross section is suppressed by a nuclear attenuation factor. For the color-octet incident gluon the attenuation is stronger than the one for the color-triplet quark, $\mathsf{S}[\boldsymbol{b}, \sigma_0^{(q\bar{q})}]_{qg}$; the two attenuation factors are related by

$$\mathsf{S}[\boldsymbol{b}, \sigma_0^{(gg)}]_{gg} = (\mathsf{S}[\boldsymbol{b}, \sigma_0^{(q\bar{q})}]_{qg})^{C_A/C_F}. \tag{109}$$

Here we notice that the nuclear attenuation of coherent diffraction can be identified with Bjorken's rapidity gap survival probability [16]. To this end, the relationship (109), in conjunction with an absence of similar nuclear attenuation for coherent quark-antiquark dijets in DIS, implies a strong breaking of diffractive factorization: the pattern of nuclear suppression of diffraction depends strongly on the hard subprocess and one can not treat diffractive production off nuclei as a hard interaction with partons of a universal nuclear pomeron. A more detailed discussion of this issue and possible implications for diffractive processes at proton-(anti)proton colliders will be reported elsewhere.

C. Excitation of gluon-gluon dijets in symmetric octet states

It is interesting to evaluate the contribution of symmetric octets alone. Here the relevant excitation operator is

$$\begin{aligned}\frac{1}{\sqrt{2}}(\langle e_2| - \langle e_3|)\mathsf{S}[\boldsymbol{b}, \hat{\Sigma}^{(0)}](|e_2\rangle + |e_3\rangle)\frac{1}{\sqrt{2}} &= \frac{1}{2}(\mathsf{S}[\boldsymbol{b}, \Sigma_2] - \mathsf{S}[\boldsymbol{b}, \Sigma_3]) \\ &= \frac{1}{2}\mathsf{S}\Big[\boldsymbol{b}, \frac{1}{2}\Sigma_1\Big]\Big(\mathsf{S}\Big[\boldsymbol{b}, \frac{1}{2}\sigma(\boldsymbol{s})\Big]\mathsf{S}\Big[\boldsymbol{b}, \frac{1}{2}\sigma(\boldsymbol{s}+\boldsymbol{r}-\boldsymbol{r}')\Big] \\ &\quad - \mathsf{S}\Big[\boldsymbol{b}, \frac{1}{2}\sigma(\boldsymbol{s}+\boldsymbol{r})\Big]\mathsf{S}\Big[\boldsymbol{b}, \frac{1}{2}\sigma(\boldsymbol{s}-\boldsymbol{r}')\Big]\Big), \end{aligned} \tag{110}$$

which results in the cross section

$$\begin{aligned}\frac{d\sigma(g^* \to \{g_1g_2\}_{8_S})}{d^2\boldsymbol{b}dzd^2\boldsymbol{p}d^2\boldsymbol{\Delta}} &= \frac{1}{4(2\pi)^2}\int d^2\boldsymbol{\kappa}_1 d^2\boldsymbol{\kappa}_2 \delta^{(2)}(\boldsymbol{\Delta} - \boldsymbol{\kappa}_1 - \boldsymbol{\kappa}_2)\Phi_g(\boldsymbol{b}, \boldsymbol{\kappa}_1)\Phi_g(\boldsymbol{b}, \boldsymbol{\kappa}_2)|\Psi(1; z, \boldsymbol{p} - \boldsymbol{\kappa}_1) - \Psi(1; z, \boldsymbol{p} - \boldsymbol{\kappa}_2)|^2 \\ &= \frac{1}{4(2\pi)^2}\int d^2\boldsymbol{\kappa}\phi_g(\boldsymbol{b}, \boldsymbol{\kappa})\phi_g(\boldsymbol{b}, \boldsymbol{\Delta} - \boldsymbol{\kappa})|\Psi(1; z, \boldsymbol{p} - \boldsymbol{\kappa}) - \Psi(1; z, \boldsymbol{p} - \boldsymbol{\Delta} + \boldsymbol{\kappa})|^2 \\ &\quad + \frac{1}{2(2\pi)^2}\cdot \mathsf{S}\Big[\boldsymbol{b}, \frac{1}{2}\sigma_0\Big]_{gg}\phi_g(\boldsymbol{b}, \boldsymbol{\Delta})|\Psi(1; z, \boldsymbol{p}) - \Psi(1; z, \boldsymbol{p} - \boldsymbol{\Delta})|^2. \end{aligned} \tag{111}$$

Of course, the coherent diffractive excitation of the symmetric octet state is not allowed—the term $\propto \delta^{(2)}(\boldsymbol{\Delta})$ is missing in here.

D. Excitation of dijets in higher multiplets: decuplets, 27-plet, R_7

In order to isolate excitation of higher multiplets we have to evaluate the matrix element

$$\begin{aligned}&-\frac{1}{2}T(\boldsymbol{b})\int_0^1 d\beta \frac{N_c^2}{\sqrt{2}N_c}\langle e_4|\mathsf{S}[\boldsymbol{b}, (1-\beta)\hat{\Sigma}^{(0)}]\hat{\omega}\mathsf{S}[\boldsymbol{b}, \beta\hat{\Sigma}^{(0)}](|e_2\rangle + |e_3\rangle) \\ &= -\frac{N_c}{2\sqrt{2}}T(\boldsymbol{b})\int_0^1 d\beta\langle e_4|\mathsf{S}[\boldsymbol{b}, (1-\beta)\hat{\Sigma}^{(0)}]|e_4\rangle\langle e_4|\hat{\omega}|e_2\rangle\langle e_2|\mathsf{S}[\boldsymbol{b}, \beta\hat{\Sigma}^{(0)}]|e_2\rangle \\ &= \frac{1}{4}T(\boldsymbol{b})\Omega(\boldsymbol{s}, \boldsymbol{r}, \boldsymbol{r}')\int_0^1 d\beta\mathsf{S}[\boldsymbol{b}, (1-\beta)\Sigma_4]\mathsf{S}[\boldsymbol{b}, \beta\Sigma_2] \equiv \frac{1}{4}T(\boldsymbol{b})\Omega(\boldsymbol{s}, \boldsymbol{r}, \boldsymbol{r}')D_A(\boldsymbol{b}, \boldsymbol{s}, \boldsymbol{r}, \boldsymbol{r}'). \end{aligned} \tag{112}$$

Let us concentrate on the nuclear distortion factor

$$D_A(\boldsymbol{b}, \boldsymbol{s}, \boldsymbol{r}, \boldsymbol{r}') = \int_0^1 d\beta\mathsf{S}[\boldsymbol{b}, (1-\beta)\Sigma_4]\mathsf{S}[\boldsymbol{b}, \beta\Sigma_2]. \tag{113}$$

It is of precisely the same form as excitation of color-octet quark-antiquark dipoles in DIS or excitation of sextet and 15-plet quark-gluon dipoles in quark-nucleus collisions. Here Σ_2 describes the initial state interactions (ISI) in the slice $[0, \beta]$ of the nucleus, whereas Σ_4 describes the final-state interactions (FSI) in the slice $[\beta, 1]$.

Now use that fact that $\Sigma_2 = \frac{1}{2}(\Sigma_1 + \Sigma_4)$ and $\mathsf{S}[\boldsymbol{b}, \beta\Sigma_2] = \mathsf{S}[\boldsymbol{b}, \frac{1}{2}\beta\Sigma_4]\mathsf{S}[\boldsymbol{b}, \frac{1}{2}\beta\Sigma_1]$ and identify $\mathsf{S}[\boldsymbol{b}, \frac{1}{2}\beta\Sigma_1] = \mathsf{S}[\boldsymbol{b}, \beta\frac{1}{2}\sigma(\boldsymbol{r})]\mathsf{S}[\boldsymbol{b}, \beta\frac{1}{2}\sigma(\boldsymbol{r}')]$ with the coherent distortions of the gluon-gluon dipole wave function in the slice $[0, \beta]$, whereas $\mathsf{S}[\boldsymbol{b}, \frac{1}{2}\beta\Sigma_4]$ will give incoherent ISI effects in the slice $[0, \beta]$. Upon the separation of coherent distortions, both the remaining ISI and FSI cross section operators are proportional to one and the same Σ_4, so that ISI and FSI can be lumped together,

$$\mathsf{S}[\boldsymbol{b}, (1-\beta)\Sigma_4]\mathsf{S}\Big[\boldsymbol{b}, \frac{1}{2}\beta\Sigma_4\Big] = \mathsf{S}\Big[\boldsymbol{b}, \frac{1}{2}(2-\beta)\Sigma_4\Big] = \mathsf{S}\Big[\boldsymbol{b}, \frac{1}{2}\Big(\frac{C_2[27]}{C_A}(1-\beta) + \beta\Big)\Sigma_4\Big]. \tag{114}$$

Of course, in the considered large-N_c approximation we have $C_2[27] = C_2[10] = C_2[R_7] = 2C_A$; hereafter we keep $C_2[27]$ on purpose as a reminder that collective nuclear glue is a density matrix in the color space, for which reason the β dependence of the nontrivial effective slice $\frac{C_2[27]}{C_A}(1-\beta) + \beta$ is controlled by the color properties of the initial and final-state partons. For a related discussion see Ref. [6]. The same comment is relevant to the case of decuplet dijets to be considered in the next section. This gives the Fourier representation

$$D_A(\boldsymbol{b},s,\boldsymbol{r},\boldsymbol{r}') = \int_0^1 d\beta S\Big[\boldsymbol{b},\beta\frac{1}{2}\sigma(\boldsymbol{r})\Big]\mathsf{S}\Big[\boldsymbol{b},\beta\frac{1}{2}\sigma(\boldsymbol{r}')\Big]\int d^2\boldsymbol{\kappa}_1 d^2\boldsymbol{\kappa}_2 \exp[is(\boldsymbol{\kappa}_1+\boldsymbol{\kappa}_2)]\exp[i\boldsymbol{\kappa}_2(\boldsymbol{r}-\boldsymbol{r}')]$$
$$\times\int_0^1 d\beta\Phi_g\Big(\frac{C_2[27]}{C_A}(1-\beta)+\beta,\boldsymbol{b},\boldsymbol{\kappa}_1\Big)\Phi_g\Big(\frac{C_2[27]}{C_A}(1-\beta)+\beta,\boldsymbol{b},\boldsymbol{\kappa}_2\Big)$$
$$=\int_0^1 d\beta\mathsf{S}\Big[\boldsymbol{b},\beta\frac{1}{2}\sigma(\boldsymbol{r})\Big]\mathsf{S}\Big[\boldsymbol{b},\beta\frac{1}{2}\sigma(\boldsymbol{r}')\Big]\int d^2\boldsymbol{\kappa}_1 d^2\boldsymbol{\kappa}_2 d^2\boldsymbol{\kappa}_3 d^2\boldsymbol{\kappa}_4\exp[is(\boldsymbol{\kappa}_1+\boldsymbol{\kappa}_2+\boldsymbol{\kappa}_3+\boldsymbol{\kappa}_4)]$$
$$\times\exp[i(\boldsymbol{\kappa}_2+\boldsymbol{\kappa}_4)(\boldsymbol{r}-\boldsymbol{r}')]\Phi_g\Big(\frac{C_2[27]}{C_A}(1-\beta);\boldsymbol{b},\boldsymbol{\kappa}_3\Big)\Phi_g(\beta,\boldsymbol{b},\boldsymbol{\kappa}_1)\Phi_g\Big(\frac{C_2[27]}{C_A}(1-\beta);\boldsymbol{b},\boldsymbol{\kappa}_4\Big)\Phi_g(\beta,\boldsymbol{b},\boldsymbol{\kappa}_2). \tag{115}$$

The second form emphasizes the distinction between the ISI interactions (the transverse momenta $\boldsymbol{\kappa}_{1,2}$) and FSI (the transverse momenta $\boldsymbol{\kappa}_{3,4}$) which is obscured in the first, convoluted, form of the distortion factor.

That resulting dijet cross section equals

$$\frac{d\sigma(g^*\to\{g_1g_2\}_{10+\overline{10}+27+R_7})}{d^2\boldsymbol{b}dzd^2\boldsymbol{p}d^2\boldsymbol{\Delta}} = \frac{1}{8(2\pi)^2}T(\boldsymbol{b})\int_0^1 d\beta\int d^2\boldsymbol{\kappa}_4 d^2\boldsymbol{\kappa}_3 d^2\boldsymbol{\kappa}_2 d^2\boldsymbol{\kappa}_1 d^2\boldsymbol{\kappa}\,\delta^{(2)}(\boldsymbol{\Delta}-\boldsymbol{\kappa}-\boldsymbol{\kappa}_1-\boldsymbol{\kappa}_2-\boldsymbol{\kappa}_3-\boldsymbol{\kappa}_4)f(\boldsymbol{\kappa})$$
$$\times\Phi_g\Big(\frac{C_2[27]}{C_A}(1-\beta);\boldsymbol{b},\boldsymbol{\kappa}_3\Big)\Phi_g(\beta;\boldsymbol{b},\boldsymbol{\kappa}_1)\Phi_g\Big(\frac{C_2[27]}{C_A}(1-\beta);\boldsymbol{b},\boldsymbol{\kappa}_4\Big)$$
$$\times\Phi_g(\beta;\boldsymbol{b},\boldsymbol{\kappa}_2)\{|\Psi(\beta;z,\boldsymbol{p}-\boldsymbol{\kappa}_2-\boldsymbol{\kappa}_4)-\Psi(\beta;z,\boldsymbol{p}-\boldsymbol{\kappa}_2-\boldsymbol{\kappa}_4-\boldsymbol{\kappa})|^2$$
$$+|\Psi(\beta;z,\boldsymbol{p}-\boldsymbol{\kappa}_1-\boldsymbol{\kappa}_3)-\Psi(\beta;z,\boldsymbol{p}-\boldsymbol{\kappa}_1-\boldsymbol{\kappa}_3-\boldsymbol{\kappa})|^2\}$$
$$=\frac{1}{8(2\pi)^2}T(\boldsymbol{b})\int_0^1 d\beta\int d^2\boldsymbol{\kappa}d^2\boldsymbol{\kappa}_1 d^2\boldsymbol{\kappa}_2 f(\boldsymbol{\kappa})\delta^{(2)}(\boldsymbol{\Delta}-\boldsymbol{\kappa}-\boldsymbol{\kappa}_1-\boldsymbol{\kappa}_2)$$
$$\times\Phi_g\Big(\frac{C_2[27]}{C_A}(1-\beta)+\beta;\boldsymbol{b},\boldsymbol{\kappa}_1\Big)\Phi_g\Big(\frac{C_2[27]}{C_A}(1-\beta)+\beta;\boldsymbol{b},\boldsymbol{\kappa}_2\Big)$$
$$\times\{|\Psi(\beta;z,\boldsymbol{p}-\boldsymbol{\kappa}_1)-\Psi(\beta;z,\boldsymbol{p}-\boldsymbol{\kappa}_1-\boldsymbol{\kappa})|^2+|\Psi(\beta,z,\boldsymbol{p}-\boldsymbol{\kappa}_2)-\Psi(\beta,z,\boldsymbol{p}-\boldsymbol{\kappa}_2-\boldsymbol{\kappa})|^2\}. \tag{116}$$

Again, we have a full agreement with the concept of the universality classes introduced in [5,6]: the pattern of coherent distortions of the wave function and of the incoherent ISI and FSI distortions repeats that of other processes with excitation of dijets in color representations with the dimension higher by the factor $\propto N_c^2$ than the dimension of the color representation of the incident parton.

A brief comment on the transition to the IA is in order. Taking $\Phi_g(\frac{C_2[27]}{C_A}(1-\beta)+\beta;\boldsymbol{b},\boldsymbol{\kappa}_1)\Phi_g(\frac{C_2[27]}{C_A}(1-\beta)+\beta;\boldsymbol{b},\boldsymbol{\kappa}_2)=\delta^{(2)}(\boldsymbol{\kappa}_1)\delta^{(2)}(\boldsymbol{\kappa}_2)$ one recovers the free-nucleon cross section times $T(\boldsymbol{b})$.

E. Excitation of decuplet dijets

The case of the decuplet dijets is exceptional because they are not excited off free nucleons via lowest order one-gluon exchange. A new feature is that intranuclear rescattering makes the production of gluon dijets in the decuplets possible and it is interesting to look at their contributions separately. Using $|10\overline{10}\rangle+|\overline{10}10\rangle=|e_4\rangle+|e_5\rangle$, the production of decuplets is induced by the excitation operator

$$-\frac{1}{2\sqrt{2}N_c}T(\boldsymbol{b})(\langle e_4|+\langle e_5|)\int_0^1 d\beta\mathsf{S}[\boldsymbol{b},(1-\beta)\hat{\Sigma}^{(0)}]\hat{\omega}\mathsf{S}[\boldsymbol{b},\beta\hat{\Sigma}^{(0)}](|e_2\rangle+|e_3\rangle)=\frac{1}{4}T(\boldsymbol{b})\Omega(\boldsymbol{s},\boldsymbol{r},\boldsymbol{r}')D^{10+\overline{10}}(\boldsymbol{b},\boldsymbol{s},\boldsymbol{r},\boldsymbol{r}'), \tag{117}$$

with the nuclear distortion factor

$$D_A^{10+\overline{10}}(\boldsymbol{b},s,\boldsymbol{r},\boldsymbol{r}')=\int_0^1 d\beta\{\langle e_4|\mathsf{S}[\boldsymbol{b},(1-\beta)\hat{\Sigma}^{(0)}]|e_4\rangle\langle e_2|\mathsf{S}[\boldsymbol{b},\beta\hat{\Sigma}^{(0)}]|e_2\rangle-\langle e_5|\mathsf{S}[\boldsymbol{b},(1-\beta)\hat{\Sigma}^{(0)}]|e_5\rangle\langle e_3|\mathsf{S}[\boldsymbol{b},\beta\hat{\Sigma}^{(0)}]|e_3\rangle\}$$
$$=\int_0^1 d\beta S\Big[\boldsymbol{b},\frac{1}{2}\beta\Sigma_1\Big]\Big\{\mathsf{S}[\boldsymbol{b},(1-\beta)\Sigma_4]\mathsf{S}\Big[\boldsymbol{b},\frac{1}{2}\beta\Sigma_4\Big]-\mathsf{S}[\boldsymbol{b},(1-\beta)\Sigma_5]\mathsf{S}\Big[\boldsymbol{b},\frac{1}{2}\beta\Sigma_5\Big]\Big\}. \tag{118}$$

The distinction between the ISI in the slice $[0, \beta]$ and FSI in the slice $[\beta, 1]$ is obvious. Repeating the analysis in the preceding section, we readily find

$$\begin{aligned} D_A^{10+\overline{10}}(\boldsymbol{b}, \boldsymbol{s}, \boldsymbol{r}, \boldsymbol{r}') &= \int_0^1 d\beta \mathsf{S}\Big[\boldsymbol{b}, \frac{1}{2}\beta\sigma(\boldsymbol{r})\Big]\mathsf{S}\Big[\boldsymbol{b}, \frac{1}{2}\beta\sigma(\boldsymbol{r}')\Big]\Big\{\mathsf{S}\Big[\boldsymbol{b}, \frac{1}{2}(2-\beta)\sigma(\boldsymbol{s})\Big]\mathsf{S}\Big[\boldsymbol{b}, \frac{1}{2}(2-\beta)\sigma(\boldsymbol{s}+\boldsymbol{r}-\boldsymbol{r}')\Big] \\ &\quad - \mathsf{S}\Big[\boldsymbol{b}, \frac{1}{2}(2-\beta)\sigma(\boldsymbol{s}+\boldsymbol{r})\Big]\mathsf{S}\Big[\boldsymbol{b}, \frac{1}{2}(2-\beta)\sigma(\boldsymbol{s}-\boldsymbol{r}')\Big]\Big\} \\ &= \int d^2\boldsymbol{\kappa}_1 d^2\boldsymbol{\kappa}_2 \exp[i(\boldsymbol{\kappa}_1+\boldsymbol{\kappa}_2)\boldsymbol{s}]\frac{1}{2}\{(\exp[i\boldsymbol{\kappa}_1\boldsymbol{r}] - \exp[i\boldsymbol{\kappa}_2\boldsymbol{r}])(\exp[-i\boldsymbol{\kappa}_1\boldsymbol{r}'] - \exp[-i\boldsymbol{\kappa}_2\boldsymbol{r}'])\} \\ &\quad \times \int_0^1 d\beta \mathsf{S}\Big[\boldsymbol{b}, \frac{1}{2}\beta\sigma(\boldsymbol{r})\Big]\mathsf{S}\Big[\boldsymbol{b}, \frac{1}{2}\beta\sigma(\boldsymbol{r}')\Big]\Phi_g(2-\beta, \boldsymbol{b}, \boldsymbol{\kappa}_1)\Phi_g(2-\beta, \boldsymbol{b}, \boldsymbol{\kappa}_2). \end{aligned} \tag{119}$$

Here

$$2-\beta = \frac{C_2[10]}{C_A}(1-\beta)+\beta \tag{120}$$

and for the sake of brevity we made an explicit use of $C_2[10] = 2C_A$. The resulting contribution of the decuplet final states to the cross section can be cast two ways

$$\begin{aligned} \frac{d\sigma(g^*\to\{g_1g_2\}_{10+\overline{10}})}{d^2\boldsymbol{b}dzd^2\boldsymbol{p}d^2\boldsymbol{\Delta}} &= \frac{1}{8(2\pi)^2}T(\boldsymbol{b})\int d^2\boldsymbol{\kappa}d^2\boldsymbol{\kappa}_1 d^2\boldsymbol{\kappa}_2\,\delta^{(2)}(\boldsymbol{\kappa}+\boldsymbol{\kappa}_1+\boldsymbol{\kappa}_2-\boldsymbol{\Delta})f(\boldsymbol{\kappa})\int_0^1 d\beta\Phi_g(2-\beta, \boldsymbol{b}, \boldsymbol{\kappa}_1)\Phi_g(2-\beta, \boldsymbol{b}, \boldsymbol{\kappa}_1) \\ &\quad \times\{|\Psi(\beta, z, \boldsymbol{p}-\boldsymbol{\kappa}_2) - \Psi(\beta, z, \boldsymbol{p}-\boldsymbol{\kappa}_1)|^2 + |\Psi(\beta, z, \boldsymbol{p}-\boldsymbol{\kappa}-\boldsymbol{\kappa}_2) - \Psi(\beta, z, \boldsymbol{p}-\boldsymbol{\kappa}-\boldsymbol{\kappa}_1)|^2 \\ &\quad \times +|\Psi(\beta, z, \boldsymbol{p}-\boldsymbol{\kappa}_2) - \Psi(\beta, z, \boldsymbol{p}-\boldsymbol{\kappa}-\boldsymbol{\kappa}_2)|^2 + |\Psi(\beta, z, \boldsymbol{p}-\boldsymbol{\kappa}_1) - \Psi(\beta, z, \boldsymbol{p}-\boldsymbol{\kappa}-\boldsymbol{\kappa}_1)|^2 \\ &\quad \times -|\Psi(\beta, z, \boldsymbol{p}-\boldsymbol{\kappa}_2) - \Psi(\beta, z, \boldsymbol{p}-\boldsymbol{\kappa}-\boldsymbol{\kappa}_1)|^2 - |\Psi(\beta, z, \boldsymbol{p}-\boldsymbol{\kappa}_1) - \Psi(\beta, z, \boldsymbol{p}-\boldsymbol{\kappa}-\boldsymbol{\kappa}_2)|^2\} \\ &= \frac{1}{8(2\pi)^2}T(\boldsymbol{b})\int d^2\boldsymbol{\kappa}d^2\boldsymbol{\kappa}_1 d^2\boldsymbol{\kappa}_2\delta^{(2)}(\boldsymbol{\kappa}+\boldsymbol{\kappa}_1+\boldsymbol{\kappa}_2-\boldsymbol{\Delta})f(\boldsymbol{\kappa})\int_0^1 d\beta\Phi_g(2-\beta, \boldsymbol{b}, \boldsymbol{\kappa}_1) \\ &\quad \times\Phi_g(2-\beta, \boldsymbol{b}, \boldsymbol{\kappa}_2)|\Psi(\beta, z, \boldsymbol{p}-\boldsymbol{\kappa}_1) - \Psi(\beta, z, \boldsymbol{p}-\boldsymbol{\kappa}_2) - \Psi(\beta, z, \boldsymbol{p}-\boldsymbol{\kappa}-\boldsymbol{\kappa}_1) \\ &\quad + \Psi(\beta, z, \boldsymbol{p}-\boldsymbol{\kappa}-\boldsymbol{\kappa}_2)|^2. \end{aligned} \tag{121}$$

Notice how the IA contribution from the term $\mathsf{S}^2[\boldsymbol{b}, \frac{1}{2}(2-\beta)\sigma_0]\delta^{(2)}(\boldsymbol{\kappa}_1)\delta^{(2)}(\boldsymbol{\kappa}_2)$ in the product $\Phi_g(2-\beta, \boldsymbol{b}, \boldsymbol{\kappa}_1)\Phi_g(2-\beta, \boldsymbol{b}, \boldsymbol{\kappa}_2)$ vanishes in accordance to the absence of the decuplet excitation off the free-nucleon target.

The production of the decuplet digluon states should lead to some interesting physical consequences in the sense of the final hadron state. In Ref. [27] (see also [28,29]) it was pointed out that the process $g\to\{gg\}_{10}$ should lead to the production of baryonium states and baryon number flow over a large rapidity gap. This observation is based on the fact that in terms of the triplet color spinor indices the decuplet state is described by the color wave function with three indices Ψ^{ijk}. For this reason the color neutralization of the decuplet state during the hadronization stage requires picking up from the vacuum three antiquarks (if one neglects purely gluon color neutralization which should be strongly suppressed as compared to the light quark mechanism due to a large effective gluon mass in the QCD vacuum $m_g^{\rm eff}\sim R_c^{-1}$, where $R_c\sim 0.27$ fm is the gluon correlation radius in the vacuum [30]). In the string model [31] the hadronization proceeds through the breaking of the triplet color strings (three strings for the decuplet state) due to Schwinger production of $q\bar{q}$ pairs in the color-electric field of the triplet strings [32].[3] For the decuplet digluon state the baryon number $N_B = -1$ will be compensated by production of an additional baryon in the nucleus fragmentation region. In the case of the antidecuplet state we have $N_B = 1$ in the digluon rapidity region, which can be viewed as a flow of valence baryon number from the nucleus region to the digluon region. This effect may be important for the baryon stopping in pA and AA collisions. The corresponding numerical estimates will be given elsewhere. In Ref. [34] it was pointed out that a similar mechanism with gluon splitting into color-decuplet/antidecuplet digluon states in the quark-gluon plasma produced in the initial stage of AA collisions should increase the high-p_T baryon production in ultrarelativistic heavy ion collisions. Numerical calculations [35] show that this mechanism (and the processes $q\to\{qg\}_{\bar{6}}$ and $\bar{q}\to\{\bar{q}g\}_6$, discussed in [6], which also lead to baryon production) may really play an important role in the anomalously

[3]In the string model for $N_c = 3$ a baryon is usually described by the Y configuration of three triplet strings connected in the so-called string junction, which plays the role of a carrier of the baryon number [33]. The baryonium state is a system of junction-antijunction connected by three triplet color strings.

large baryon/meson ratio observed experimentally at RHIC (for the recent review see [36]).

F. Excitation of color-singlet dijets

Excitation of the color-singlet gluon-gluon dijets is a N_c-suppressed process. Still it is an interesting example of a reaction in which the incident parton in the higher multiplet excites a dijet in a lower color multiplet. The relevant matrix element of the off-diagonal transition operator (84) equals

$$\begin{aligned}\langle e_1|\mathsf{S}[\boldsymbol{b}, \hat{\sigma}^{(4)}(\boldsymbol{s},\boldsymbol{r},\boldsymbol{r}')]|in\rangle &= \frac{1}{4N_c^2}\Omega(\boldsymbol{s},\boldsymbol{r},\boldsymbol{r}')T(\boldsymbol{b})\int_0^1 d\beta \mathsf{S}[\boldsymbol{b},(1-\beta)\Sigma_1]\Big\{\mathsf{S}\Big[\boldsymbol{b},\beta\Sigma_2\Big]+\mathsf{S}\Big[\boldsymbol{b},\beta\Sigma_3\Big]\Big\}\\ &= \frac{1}{4N_c^2}\Omega(\boldsymbol{s},\boldsymbol{r},\boldsymbol{r}')T(\boldsymbol{b})\int_0^1 d\beta \mathsf{S}\Big[\boldsymbol{b},\Big[(1-\beta)+\frac{1}{2}\beta\Big]\sigma(\boldsymbol{r})\Big]\mathsf{S}\Big[\boldsymbol{b},\Big[(1-\beta)+\frac{1}{2}\beta\Big]\sigma(\boldsymbol{r}')\Big]\\ &\quad\times\Big\{\mathsf{S}\Big[\boldsymbol{b},\frac{1}{2}\beta\sigma(\boldsymbol{s})\Big]\mathsf{S}\Big[\boldsymbol{b},\frac{1}{2}\beta\sigma(\boldsymbol{s}+\boldsymbol{r}-\boldsymbol{r}')\Big]+\mathsf{S}\Big[\boldsymbol{b},\frac{1}{2}\beta\sigma(\boldsymbol{s}+\boldsymbol{r})\Big]\mathsf{S}\Big[\boldsymbol{b},\frac{1}{2}\beta\sigma(\boldsymbol{s}-\boldsymbol{r}')\Big]\Big\}\\ &= \frac{1}{4N_c^2}\Omega(\boldsymbol{s},\boldsymbol{r},\boldsymbol{r}')T(\boldsymbol{b})\int d^2\boldsymbol{\kappa}_1 d^2\boldsymbol{\kappa}_2\exp[i(\boldsymbol{\kappa}_1+\boldsymbol{\kappa}_2)\boldsymbol{s}]\frac{1}{2}\{(\exp[i\boldsymbol{\kappa}_1\boldsymbol{r}]\\ &\quad+\exp[i\boldsymbol{\kappa}_2\boldsymbol{r}])(\exp[-i\boldsymbol{\kappa}_1\boldsymbol{r}']+\exp[-i\boldsymbol{\kappa}_2\boldsymbol{r}'])\}\int_0^1 d\beta\mathsf{S}\Big[\boldsymbol{b},\Big[(1-\beta)+\frac{1}{2}\beta\Big]\sigma(\boldsymbol{r})\Big]\\ &\quad\times\mathsf{S}\Big[\boldsymbol{b},\Big[(1-\beta)+\frac{1}{2}\beta\Big]\sigma(\boldsymbol{r}')\Big]\Phi_g\Big(\frac{1}{2}\beta,\boldsymbol{b},\boldsymbol{\kappa}_1\Big)\Phi_g\Big(\frac{1}{2}\beta,\boldsymbol{b},\boldsymbol{\kappa}_2\Big).\end{aligned} \tag{122}$$

We immediately recognize the coherent distortion factors $\mathsf{S}[\boldsymbol{b},[(1-\beta)+\frac{1}{2}\beta]\sigma(\boldsymbol{r})]$ and $\mathsf{S}[\boldsymbol{b},[(1-\beta)+\frac{1}{2}\beta]\sigma(\boldsymbol{r}')]$—interestingly, the coherent distortion is picked up over the whole nucleus, with different strength from the ISI and FSI. The corresponding dijet spectrum reads

$$\begin{aligned}\frac{d\sigma(g^*\to\{g_1g_2\}_1)}{d^2\boldsymbol{b}dzd^2\boldsymbol{p}d^2\boldsymbol{\Delta}} &= \frac{1}{8N_c^2(2\pi)^2}T(\boldsymbol{b})\int d^2\boldsymbol{\kappa}d^2\boldsymbol{\kappa}_1d^2\boldsymbol{\kappa}_2\delta^{(2)}(\boldsymbol{\kappa}+\boldsymbol{\kappa}_1+\boldsymbol{\kappa}_2-\boldsymbol{\Delta})f(\boldsymbol{\kappa})\\ &\quad\times\int_0^1 d\beta\Phi_g\Big(\frac{1}{2}\beta,\boldsymbol{b},\boldsymbol{\kappa}_1\Big)\Phi_g\Big(\frac{1}{2}\beta,\boldsymbol{b},\boldsymbol{\kappa}_2\Big)|\Psi(2(1-\beta)+\beta,z,\boldsymbol{p}-\boldsymbol{\kappa}_1)+\Psi(2(1-\beta)+\beta,z,\boldsymbol{p}-\boldsymbol{\kappa}_2)\\ &\quad-\Psi(2(1-\beta)+\beta,z,\boldsymbol{p}-\boldsymbol{\kappa}-\boldsymbol{\kappa}_1)-\Psi(2(1-\beta)+\beta,z,\boldsymbol{p}-\boldsymbol{\kappa}-\boldsymbol{\kappa}_2)|^2.\end{aligned} \tag{123}$$

G. Mini summary and comparison with other works on gluon-gluon dijets

A brief summary of technical aspects of our approach and a comparison with the related recent works by Jalilian-Marian and Kovchegov [14] and Baier *et al.* [15] is in order. Our work starts with the extension of the Glauber-Gribov multiple-scattering theory to hard interactions of color dipoles with nuclei. The application of closure to the dijet cross sections inclusive over all final states of the target (nucleon, nucleus) gives rise to our master formula (11) in terms of the S matrices for multiparton states. The works of Refs. [14,15] use the Wilson-line representation for S matrices in the large-N_c limit. After the application of nuclear closure, they calculate nuclear expectation values of products of Wilson lines under certain assumptions on the gluon field correlators. At this point one can establish an one-to-one correspondence between our nuclear S matrices for multiparton states and nuclear averages of products of Wilson lines; the marginal difference is in the heavy use of a specific parameterization for the dipole cross section in Refs. [14,15].

For the further comparison we depart from our integral representation (85) and apply to $\mathsf{S}[\boldsymbol{b},\hat{\sigma}^{(4)}(\boldsymbol{s},\boldsymbol{r},\boldsymbol{r}')]$ the Sylvester expansion [2,4]. Truncated to terms which contribute to transitions from the initial state (81) to the final state (80), to the leading order of large-N_c perturbation theory, it reads

$$\begin{aligned}\mathsf{S}[\boldsymbol{b},\hat{\sigma}^{(4)}(\boldsymbol{s},\boldsymbol{r},\boldsymbol{r}')] &= |e_2\rangle\langle e_2|\exp\Big[-\frac{1}{2}\Sigma_2T(\boldsymbol{b})\Big]\\ &\quad+|e_4\rangle\langle e_2|\frac{\Omega(\boldsymbol{s},\boldsymbol{r},\boldsymbol{r}')}{\sqrt{2}N_c(\Sigma_2-\Sigma_4)}\\ &\quad\times\Big\{\exp\Big[-\frac{1}{2}\Sigma_4T(\boldsymbol{b})\Big]\\ &\quad-\exp\Big[-\frac{1}{2}\Sigma_2T(\boldsymbol{b})\Big]\Big\}.\end{aligned} \tag{124}$$

The matrix element of (124) between the initial and final states, in conjunction with the contribution from two-parton and three-parton S matrices, gives the same result for the color-dipole representation for the digluon spectrum in $g \to gg$ as the one which enters the discussion of $qA \to qggX$ reaction in Refs. [14,15]. In contrast to our integral representation (85), which enabled us to cast all the dijet spectra in an analytic form as quadratures of the collective nuclear glue, the denominator $(\Sigma_2 - \Sigma_4)$ in the Sylvester expansion (124) blocks further analytic calculations. Here one has to rely upon the brute force numerical Fourier transform. Our explicit separation of cross sections for dijets in different color representation sheds further light on the diversity of production mechanisms, for instance, the identification of final states described by the in-nucleus modified fragmentation functions [4–6]. Finally, our integral representation (85) makes obvious the fundamental difference between the coherent and incoherent initial- and final-state interactions. It clarifies also the origin of the nonlinearity of nuclear S matrices in terms of S matrices for elementary dipoles, by which nonlinear $k_\perp$ factorization becomes an indispensable feature of the pQCD description of hard processes in a nuclear environment.

VII. CONCLUSIONS

We derived the nonlinear $k_\perp$ factorization for the last missing pQCD subprocess—production of hard gluon-gluon dijets in gluon-nucleus collisions when the nuclear coherency condition $x \lesssim x_A \approx 0.1 \cdot A^{-1/3}$ holds. Although of limited importance at the not so high energies of RHIC, this subprocess will be a dominant source of midrapidity and proton-hemisphere dijets in pA collisions at LHC. The principal technical novelty is a solution of the rather involved seven-channel non-Abelian evolution equations for intranuclear propagation of four-gluon states. Our results for the gluon-gluon dijets in all color representations are presented in the form of explicit quadratures. The concept of universality classes [5,6] is fully corroborated. The nonlinear $k_\perp$ factorization properties of excitation of digluons in higher color representations are identical to those in excitation of color-octet quark-antiquark dijets in DIS and quark-gluon dijets in higher color representations in qA collisions. The manifest distinction between the initial state and final-state interaction effects, inherent to this universality class, requires a description in terms of collective nuclear glue defined for slices of a nucleus—nonlinear $k_\perp$ factorization cannot be described by the classical gluon field of the whole nucleus. Similar nonlinear $k_\perp$ factorization properties are exhibited by excitation of dijets in the same color representation as the incident parton: $g \to \{gg\}_8$, $g \to \{q\bar{q}\}_8$, $q \to \{qg\}_3$—this universality class admits an interpretation of the hard fragmentation of scattered partons with the in-nucleus modified fragmentation function. In both $g \to gg$ and $q \to qg$ processes coherent diffractive excitation of incident partons with net color charge is suppressed by a nuclear absorption factor which can be identified with Bjorken's gap survival probability. The gap survival probabilities in the two cases are different. Furthermore, the related absorption is absent in diffractive $\gamma^* \to q\bar{q}$, which is indicative of a strong breaking of diffractive factorization. We mentioned midrapidity to proton-hemisphere gluon-gluon dijets in pA collisions at LHC as a future application of the derived formalism. Still another potential application of our results for color-decuplet digluon production is a baryon number flow from the nucleus to large rapidity region. But, first and foremost, this work completes a derivation of nonlinear $k_\perp$ factorization for all pQCD processes in a nuclear medium and opens a way to systematic comparative studies of high-$p_\perp$ jet-jet and hadron-hadron correlations in different parts of the phase space of DIS off nuclei and hadron-nucleus collisions.

The diagonalization properties of the single-jet problem are somewhat beyond the major theme of this communication. Still, in view of the discussion in Sec. VI E the isolation of contributions from different final states is of certain interest. Correspondingly, we included Appendix C on the manifest diagonalization of the initially seven-coupled channel problem in the t-channel basis. This property is, apparently, of more general interest and may find further applications in other problems.

ACKNOWLEDGMENTS

This work was partly supported by Grants Nos. DFG 436 RUS 17/101/04 and DFG RUS 17/138/05.

APPENDIX A: USEFUL $SU(N_c)$ RELATIONS

In this appendix we collect a number of identities that are helpful in the evaluation of the matrix elements of the dipole cross section operator. In the derivation of the projectors we follow closely, though in slightly different notation and normalization, Ref. [26]. Many useful $SU(N_c)$ identities can be found in Refs. [37,38].

If $t^a, a = 1 \dots N_c^2 - 1$ are $SU(N_c)$ generators in the fundamental representation, the familiar f and d tensors are defined through

$$t^a t^b = \frac{1}{2N_c} \delta_{ab} \mathbb{1} + \frac{1}{2}(d_{abc} + i f_{abc}) t^c, \qquad (A1)$$

or,

$$i f_{abc} = 2\,\mathrm{Tr}([t^a, t^b] t^c), \qquad d_{abc} = 2\,\mathrm{Tr}(\{t^a, t^b\} t^c). \quad (A2)$$

The $SU(N_c)$ generators in the adjoint representation are

$$(T^a)_{bc} = i f_{bac} \qquad (A3)$$

so that their defining property $[T^a, T^b] = i f_{abc} T^c$, and the $SU(N_c)$ transformation properties of d symbols give rise to the Jacobi identities

$$if_{kam}if_{mbl} - if_{kbm}if_{mal} = if_{abm}if_{kml}, \quad \text{(A4)}$$

$$f_{kam}d_{mbl} - d_{kbm}f_{mal} = f_{abm}d_{kml}. \quad \text{(A5)}$$

To evaluate contractions of multiple f and d symbols one makes use of the Fierz identity for the fundamental generators,

$$(t^a)^i_j(t^a)^k_l = \frac{1}{2}\delta^i_l\delta^k_j - \frac{1}{2N_c}\delta^i_j\delta^k_l. \quad \text{(A6)}$$

They entail that

$$\begin{aligned}\mathrm{Tr}(At^a)\,\mathrm{Tr}(Bt^a) &= \frac{1}{2}\,\mathrm{Tr}(AB) - \frac{1}{2N_c}\,\mathrm{Tr}(A)\,\mathrm{Tr}(B),\\ \mathrm{Tr}(At^aBt^a) &= \frac{1}{2}\,\mathrm{Tr}(A)\,\mathrm{Tr}(B) - \frac{1}{2N_c}\,\mathrm{Tr}(AB).\end{aligned} \quad \text{(A7)}$$

In conjunction with Eq. (A2) one can then obtain

$$f_{aij}f_{bij} = N_c\delta_{ab}, \qquad d_{aij}d_{bij} = \frac{N_c^2-4}{N_c}\delta_{ab}, \qquad f_{aij}d_{bij} = 0; \quad \text{(A8)}$$

$$\begin{aligned}&f_{iaj}f_{jbk}f_{kci} = -\frac{N_c}{2}f_{abc}, \qquad f_{iaj}f_{jbk}d_{kci} = -\frac{N_c}{2}d_{abc}, \qquad f_{iaj}d_{jbk}d_{kci} = \frac{N_c^2-4}{2N_c}f_{abc},\\ &d_{iaj}d_{jbk}d_{kci} = \frac{N_c^2-12}{2N_c}d_{abc}.\end{aligned} \quad \text{(A9)}$$

$$\begin{aligned}f_{kan}f_{nbm}f_{mdl}f_{lck} &= \delta_{ac}\delta_{bd} + \delta_{ab}\delta_{cd} + \frac{N_c}{4}(d_{ack}d_{kdb} + d_{abk}d_{kcd} - d_{adk}d_{kbc}),\\ d_{kan}d_{nbm}d_{mdl}d_{lck} &= \frac{N_c^2-4}{N_c^2}(\delta_{ac}\delta_{bd} + \delta_{ab}\delta_{cd}) + \frac{N_c^2-16}{4N_c}(d_{ack}d_{kdb} + d_{abk}d_{kcd}) - \frac{N_c}{4}d_{adk}d_{kcb}.\end{aligned} \quad \text{(A10)}$$

It is helpful to analyze the box and twisted-box traces of four fundamental generators,

$$R^{ab}_{cd} \equiv 4\,\mathrm{Tr}(t^at^bt^dt^c), \qquad Q^{ab}_{cd} = 4\,\mathrm{Tr}(t^at^dt^bt^c). \quad \text{(A11)}$$

From Eq. (A1), we obtain immediately

$$\begin{aligned}R^{ab}_{cd} &= \frac{1}{N_c}\delta_{ab}\delta_{cd} + \frac{1}{2}(d_{abk}d_{kdc} + if_{abk}if_{kdc})\\ &\quad + \frac{i}{2}(d_{abk}f_{kdc} + f_{abk}d_{kdc}),\end{aligned} \quad \text{(A12)}$$

on the other hand,

$$R^{ab}_{cd} \equiv 4\,\mathrm{Tr}(t^at^bt^dt^c) = 4\,\mathrm{Tr}(t^ct^at^bt^d), \quad \text{(A13)}$$

so that also

$$\begin{aligned}R^{ab}_{cd} &= \frac{1}{N_c}\delta_{ac}\delta_{bd} + \frac{1}{2}(d_{cak}d_{kbd} + if_{cak}if_{kbd})\\ &\quad + \frac{i}{2}(d_{cak}f_{kbd} + f_{cak}d_{kbd}).\end{aligned} \quad \text{(A14)}$$

We can equate the real and imaginary parts of R from Eqs. (A12) and (A14) separately, and thus obtain the identities

$$d_{abk}f_{kdc} + f_{abk}d_{kdc} = d_{cak}f_{kbd} + f_{cak}d_{kbd}, \quad \text{(A15)}$$

$$\begin{aligned}&\frac{2}{N_c}(\delta_{ac}\delta_{bd} - \delta_{ab}\delta_{cd}) + d_{cak}d_{kbd} - d_{abk}d_{kdc}\\ &\quad = if_{abk}if_{kdc} - if_{cak}if_{kbd} = if_{adk}if_{kbc}.\end{aligned} \quad \text{(A16)}$$

For the tensor Q we have

$$\begin{aligned}Q^{ab}_{cd} &= \frac{1}{N_c}\delta_{ad}\delta_{bc} + \frac{1}{2}(d_{adk}d_{kbc} + if_{adk}if_{kbc})\\ &\quad + \frac{i}{2}(d_{adk}f_{kbc} + f_{adk}d_{kbc})\\ &= \frac{1}{N_c}(\delta_{ad}\delta_{bc} + \delta_{ac}\delta_{bd} - \delta_{ab}\delta_{cd})\\ &\quad + \frac{1}{2}(d_{adk}d_{kbc} + d_{cak}d_{kbd} - d_{abk}d_{kdc}) + iY^{ab}_{cd},\end{aligned} \quad \text{(A17)}$$

where we introduced a shorthand notation

$$iY^{ab}_{cd} = \frac{i}{2}(d_{adk}f_{kbc} + f_{adk}d_{kbc}) = \frac{i}{2}(f_{cak}d_{kdb} + d_{cak}f_{kdb}), \quad \text{(A18)}$$

and made use of Eqs. (A15) and (A16).

APPENDIX B: DERIVATION OF THE PROJECTORS ONTO IRREDUCIBLE REPRESENTATIONS

Our task is now to find the irreducible representations (29) for the product of two adjoints and to construct the relevant projection operators. The auxiliary tensors

$$S^{ab}_{cd} \equiv \frac{1}{2}(\delta_{ac}\delta_{bd} + \delta_{ad}\delta_{bc}), \quad \mathcal{A}^{ab}_{cd} \equiv \frac{1}{2}(\delta_{ac}\delta_{bd} - \delta_{ad}\delta_{bc}) \quad \text{(B1)}$$

decompose the product representation space into its symmetric and antisymmetric parts, respectively:

$$\mathbb{1}^{ab}_{cd} \equiv \delta_{ac}\delta_{bd} = S^{ab}_{cd} + \mathcal{A}^{ab}_{cd}. \quad \text{(B2)}$$

In addition, also

$$[D_t]^{ab}_{cd} \equiv d_{ack}d_{kbd}, \qquad [D_u]^{ab}_{cd} \equiv d_{adk}d_{kbc}, \qquad [D_s]^{ab}_{cd} \equiv d_{abk}d_{kcd} \quad \text{(B3)}$$

will prove helpful. All the above defined tensors S, $\mathcal{A}$, D_s, D_t, D_u, as well as iY of Eq. (A18) are Hermitian, i.e. $(\mathcal{O}^\dagger)^{ab}_{cd} = (\mathcal{O}^{cd}_{ab})^* = \mathcal{O}^{ab}_{cd}$. The $SU(N_c)$ projectors onto the singlet as well as the two adjoint multiplets have up to the normalization factors manifestly the same form as their well-known $N_c = 3$ counterparts.

$$P[1]^{ab}_{cd} = \frac{1}{N_c^2 - 1}\delta_{ab}\delta_{cd}, \quad \text{(B4)}$$

$$P[8_S]^{ab}_{cd} = \frac{N_c}{N_c^2 - 4}d_{abk}d_{kcd} = \frac{N_c}{N_c^2 - 4}[D_s]^{ab}_{cd} \quad \text{(B5)}$$

project onto the symmetric singlet and octet, respectively, while

$$P[8_A]^{ab}_{cd} = \frac{1}{N_c}f_{abk}f_{kcd} = \frac{1}{N_c}if_{abk}if_{kdc} \quad \text{(B6)}$$

projects onto the antisymmetric octet. It is easily checked that they are indeed Hermitian and satisfy the requirement

$$(P[R_i]^2)^{ab}_{cd} = P[R_i]^{ab}_{kl}P[R_i]^{kl}_{cd} = P[R_i]^{ab}_{cd}. \quad \text{(B7)}$$

Using the identities (A9) and (A10), one finds the number of states they propagate:

$$\mathrm{Tr}\, P[R_i] \equiv P[R_i]^{ab}_{ab} = \dim[R_i], \quad \text{(B8)}$$

explicitly,

$$\mathrm{Tr}\, P[1] = 1, \qquad \mathrm{Tr} P[8_A] = \mathrm{Tr} P[8_S] = N_c^2 - 1. \quad \text{(B9)}$$

The symmetric and antisymmetric parts of our space contain, respectively,

$$\mathrm{Tr}\, S = \tfrac{1}{2}N_c^2(N_c^2 - 1), \qquad \mathrm{Tr}\mathcal{A} = \tfrac{1}{2}(N_c^2 - 1)(N_c^2 - 2) \quad \text{(B10)}$$

states, so that now the problem arises to find the decomposition into irreducible representations of the subspaces that belong to the projectors

$$S_\perp = S - P[1] - P[8_S], \qquad \mathcal{A}_\perp = \mathcal{A} - P[8_A]. \quad \text{(B11)}$$

This is done most straightforwardly, following [26], by investigating the above defined tensor Q (A17), which takes the form

$$Q = \frac{2}{N_c}S - \frac{N_c^2 - 1}{N_c}P[1] - \frac{N_c^2 - 4}{2N_c}P[8_S] + \frac{1}{2}(D_u + D_t) + iY. \quad \text{(B12)}$$

First notice that its symmetric (antisymmetric) part is purely real (imaginary),

$$SQS = \Re e Q, \qquad \mathcal{A}Q\mathcal{A} = i\Im m Q, \quad \text{(B13)}$$

and furthermore

$$SQS = SQ = QS, \qquad \mathcal{A}Q\mathcal{A} = \mathcal{A}Q = Q\mathcal{A}. \quad \text{(B14)}$$

Now evaluate its square, Q^2—best by starting from its definition as a trace of fundamental generators—

$$\begin{aligned}(Q^2)^{ab}_{cd} &= 16\,\mathrm{Tr}(t^a t^l t^b t^k)\,\mathrm{Tr}(t^k t^d t^l t^c) \\ &= 4\,\mathrm{Tr}(t^a t^c)\,\mathrm{Tr}(t^b t^d) + \frac{4}{N_c^2}\,\mathrm{Tr}(t^c t^d)\,\mathrm{Tr}(t^a t^b) \\ &\quad - \frac{4}{N_c}(\mathrm{Tr}(t^a t^b t^d t^c) + \mathrm{Tr}(t^c t^d t^b t^a)) \\ &= \delta_{ac}\delta_{bd} + \frac{1}{N_c^2}\delta_{cd}\delta_{ab} - \frac{2}{N_c}\Re e R^{cd}_{ab},\end{aligned} \quad \text{(B15)}$$

so that

$$Q^2 = \mathbb{1} - \frac{N_c^2 - 1}{N_c^2}P[1] - \frac{N_c^2 - 4}{N_c^2}P[8_S] - P[8_A]. \quad \text{(B16)}$$

From here we can conclude that on the subspaces under investigation, Q^2 acts as the unit matrix:

$$S_\perp Q^2 = Q^2 S_\perp = S_\perp, \qquad \mathcal{A}_\perp Q^2 = Q^2 \mathcal{A}_\perp = \mathcal{A}_\perp, \tag{B17}$$

therefore both subspaces decompose into orthogonal eigen-spaces belonging to eigenvalues ± 1 of the operator Q. We can then write down the projection operators

$$P^{\pm}_{A_\perp} = \tfrac{1}{2}(\mathbb{1} \pm Q)\mathcal{A}_\perp = \tfrac{1}{2}(\mathbb{1} \pm i\Im m Q)\mathcal{A}_\perp, \tag{B18}$$

$$P^{\pm}_{S_\perp} = \tfrac{1}{2}(\mathbb{1} \pm Q)S_\perp = \tfrac{1}{2}(\mathbb{1} \pm \Re e Q)S_\perp. \tag{B19}$$

To evaluate the dimensions of the associated representations, we first derive more explicit forms of the projectors. We start with the symmetric case. From the relations (A9) and (A10), we obtain

$$\begin{aligned}(D_u + D_t)P[1] &= \frac{2(N_c^2 - 4)}{N_c} P[1],\\ (D_u + D_t)P[8_S] &= \frac{N_c^2 - 12}{N_c} P[8_S],\end{aligned} \tag{B20}$$

and, trivially,

$$(D_u + D_t)S = D_u + D_t, \tag{B21}$$

so that

$$\begin{aligned}P^{\pm}_{S_\perp} &= \frac{1}{2}\bigg\{\bigg(1 \pm \frac{2}{N_c}\bigg)S_\perp \pm \frac{1}{2}(D_u + D_t) \mp \frac{N_c^2 - 4}{N_c}P[1]\\ &\quad \mp \frac{N_c^2 - 12}{2N_c}P[8_S]\bigg\}\\ &= \frac{1}{2}\bigg\{(1 \pm \frac{2}{N_c})S \mp \frac{(N_c \pm 2)(N_c \mp 1)}{N_c}P[1]\\ &\quad \mp \frac{(N_c \mp 2)(N_c \pm 4)}{2N_c}P[8_S] \pm \frac{1}{2}(D_u + D_t)\bigg\}.\end{aligned} \tag{B22}$$

Now,

$$\mathrm{Tr}\, D_t = 0, \qquad \mathrm{Tr} D_u = \frac{(N_c^2 - 4)(N_c^2 - 1)}{N_c}, \tag{B23}$$

so that we can easily establish that

$$\begin{aligned}\mathrm{Tr}\, P^{+}_{S_\perp} &= \frac{N_c^2(N_c - 1)(N_c + 3)}{4},\\ \mathrm{Tr} P^{-}_{S_\perp} &= \frac{N_c^2(N_c + 1)(N_c - 3)}{4}.\end{aligned} \tag{B24}$$

For $N = 3$, we have

$$\mathrm{Tr}\, P^{+}_{S_\perp}|_{N_c=3} = 27, \qquad \mathrm{Tr} P^{-}_{S_\perp}|_{N_c=3} = 0, \tag{B25}$$

so that from now on we shall denote $P^{+}_{S_\perp} \equiv P[27]$, whereas for the other symmetric representation, which vanishes for $N_c = 3$ we shall use the notation $P^{-}_{S_\perp} \equiv P[R_7]$. It is interesting to note that the vanishing of R_7 for three colors can be related to a well-known accidental cancellation, namely,

$$\begin{aligned}P[R_7]^{ab}_{cd}|_{N_c=3} = \tfrac{1}{4}\{\tfrac{1}{3}(\delta_{ac}\delta_{bd} + \delta_{ad}\delta_{bc} + \delta_{ab}\delta_{cd})\\ - (d_{ack}d_{kbd} + d_{adk}d_{kbc} + d_{abk}d_{kcd})\},\end{aligned} \tag{B26}$$

is identically zero for $SU(3)$ [37].

This completes the reduction of the symmetric part, where we have

$$S = P[1] + P[8_S] + P[27] + P[R_7]. \tag{B27}$$

We now turn to the antisymmetric part of the product representation space, where we deal with two complex conjugate multiplets. Here we see that

$$QP[8_A] = i\Im m Q P[8_A] = iYP[8_A] = 0, \tag{B28}$$

and hence

$$\begin{aligned}P^{\pm}_{A_\perp} &= \tfrac{1}{2}(\mathbb{1} \pm Q)\mathcal{A}_\perp = \tfrac{1}{2}(\mathbb{1} \pm i\Im m Q)\mathcal{A}_\perp\\ &= \tfrac{1}{2}(\mathcal{A} - P[8_A] \pm iY).\end{aligned} \tag{B29}$$

As $\mathrm{Tr} iY = 0$, we have

$$\mathrm{Tr}\, P^{\pm}_{A_\perp} = \frac{(N_c^2 - 1)(N_c^2 - 4)}{4}, \tag{B30}$$

for $SU(3)$

$$\mathrm{Tr}\, P^{\pm}_{A_\perp}|_{N_c=3} = 10, \tag{B31}$$

so that from now on

$$P^{+}_{A_\perp} \equiv P[10], P^{-}_{A_\perp} \equiv P[\overline{10}]. \tag{B32}$$

Of course in this context it is merely a convention which multiplet we address as the decuplet and which as the antidecuplet. This completes our reduction of the antisymmetric part,

$$\mathcal{A} = P[8_A] + P[10] + P[\overline{10}]. \tag{B33}$$

APPENDIX C: EIGENSTATES FOR THE SINGLE-PARTICLE PROBLEM AND THE CROSSING MATRIX

In the general case, a classification of the independent color states of the four-parton state $ab\bar{c}\,\bar{d}$ amounts to the determination of independent amplitudes in the scattering process $ab \to cd$. In Sec. IV we computed the dipole cross section operator in the s-channel basis of states where gluons $1, 2$ and $1', 2'$, respectively, were in a definite $SU(N_c)$ multiplet. For the remainder of this section let us denote these states by $|R\overline{R}\rangle_s$:

$$|R\overline{R}\rangle_s \equiv |\{[g^a(\boldsymbol{b}_1)\otimes g^b(\boldsymbol{b}_2)]_R \otimes [g^c(\boldsymbol{b}_1')\otimes g^d(\boldsymbol{b}_2')]_{\overline{R}}\}_1\rangle = \frac{1}{\sqrt{\dim[R]}} P[R]^{ab}_{cd} |g^a(\boldsymbol{b}_1)\otimes g^b(\boldsymbol{b}_2)\otimes g^c(\boldsymbol{b}_1')\otimes g^d(\boldsymbol{b}_2')\rangle. \tag{C1}$$

We mentioned that for purposes of the single-particle spectrum and total cross section, the dipole cross section operator is diagonalized in the t-channel basis where gluons $1, 1'$ and $2, 2'$, respectively, are in definite color multiplets; we shall denote this basis by $|R\overline{R}\rangle_t$:

$$|R\overline{R}\rangle_t \equiv |\{[g^a(\boldsymbol{b}_1)\otimes g^c(\boldsymbol{b}_1')]_R \otimes [g^b(\boldsymbol{b}_2)\otimes g^d(\boldsymbol{b}_2')]_{\overline{R}}\}_1\rangle = \frac{1}{\sqrt{\dim[R]}} P[R]^{ac}_{bd} |g^a(\boldsymbol{b}_1)\otimes g^b(\boldsymbol{b}_2)\otimes g^c(\boldsymbol{b}_1')\otimes g^d(\boldsymbol{b}_2')\rangle. \tag{C2}$$

The proof that the basis (C2) indeed diagonalizes the dipole cross section operator of the single-particle spectrum proceeds as follows: First, the dipole cross section matrix with respect to the basis (C2) is obtained from the one with respect to (C1) by the swap of impact parameters

$$\{\boldsymbol{b}_1, \boldsymbol{b}_2, \boldsymbol{b}_1', \boldsymbol{b}_2'\} \rightarrow \{\boldsymbol{b}_1, \boldsymbol{b}_1', \boldsymbol{b}_2, \boldsymbol{b}_2'\}. \tag{C3}$$

That means, for the off-diagonal piece we obtain

$$t\langle R'\overline{R'}|\hat{\sigma}^{(4)}|R\overline{R}\rangle_t \propto \Omega(\boldsymbol{b}_1, \boldsymbol{b}_1', \boldsymbol{b}_2, \boldsymbol{b}_2') = \sigma(\boldsymbol{b}_1' - \boldsymbol{b}_2) + \sigma(\boldsymbol{b}_1 - \boldsymbol{b}_2') - \sigma(\boldsymbol{b}_1 - \boldsymbol{b}_2) - \sigma(\boldsymbol{b}_1' - \boldsymbol{b}_2'). \tag{C4}$$

Now, for the single-particle spectrum, one would integrate out, say $\boldsymbol{p}2$ in the master formula (13), and in effect put $\boldsymbol{b}_2 = \boldsymbol{b}_2'$, but then,

$$\Omega(\boldsymbol{b}_1, \boldsymbol{b}_1', \boldsymbol{b}_2, \boldsymbol{b}_2) \equiv 0. \tag{C5}$$

Hence, for the purposes of the single-particle spectrum, the off-diagonal elements of the dipole cross section vanish identically in the basis of states $|R\overline{R}\rangle_t$, which is what we set out to prove.

As the dipole cross section matrix in the basis (C2) is obtained from the simple swap (C3), we can immediately give its eigenvalues λ_i:

$$\begin{aligned}
\lambda_1 &= \sigma(\boldsymbol{r} - \boldsymbol{r}'),\\
\lambda_2 &= \lambda_3 = \frac{1}{2}[\sigma(\boldsymbol{r}) + \sigma(\boldsymbol{r}') + \sigma(\boldsymbol{r} - \boldsymbol{r}')].\\
\lambda_4 &= \lambda_5 = \sigma(\boldsymbol{r}) + \sigma(\boldsymbol{r}'),\\
\lambda_6 &= \frac{N_c + 1}{N_c}[\sigma(\boldsymbol{r}) + \sigma(\boldsymbol{r}')] - \frac{1}{N_c}\sigma(\boldsymbol{r} - \boldsymbol{r}'),\\
\lambda_7 &= \frac{N_c - 1}{N_c}[\sigma(\boldsymbol{r}) + \sigma(\boldsymbol{r}')] + \frac{1}{N_c}\sigma(\boldsymbol{r} - \boldsymbol{r}'),
\end{aligned} \tag{C6}$$

where, as throughout the main body of the text, $\boldsymbol{r} = \boldsymbol{b}_1 - \boldsymbol{b}_2$, $\boldsymbol{r}' = \boldsymbol{b}_1' - \boldsymbol{b}_2'$. The system of eigenvectors which belong to the λ_i is

$$|\lambda_1\rangle = |11\rangle_t, \quad |\lambda_2\rangle = |8_A 8_A\rangle_t, \quad |\lambda_3\rangle = |8_S 8_S\rangle_t, \quad |\lambda_4\rangle = |10\overline{10}\rangle_t, \quad |\lambda_5\rangle = |\overline{10}10\rangle_t, \quad |\lambda_6\rangle = |2727\rangle_t, \quad |\lambda_7\rangle = |R_7 R_7\rangle_t. \tag{C7}$$

Clearly, once the spectrum of a matrix is known, the Sylvester formula would allow one to calculate any function of the matrix without knowledge of the eigenstates. In practice, however, explicit knowledge of the latter is helpful. To obtain the color wave functions of the states (C2), we need to establish the Fierz-type identities:

$$P_t[R_j] = \sum_{i=1}^{9} C_i^j P_s[R_i], \tag{C8}$$

i.e.

$$P[R_j]^{ac}_{bd} = \sum_{i=1}^{9} C_i^j P[R_i]^{ab}_{cd}, \tag{C9}$$

The t-channel projectors thus read, component wise,

$$P_t[R]^{ab}_{cd} \equiv P_s[R]^{ac}_{bd}. \tag{C10}$$

The crossing matrix C_i^j is now obtained as (for a diagrammatic representation, see Fig. 7)

$$C_i^j = \frac{P[R_j]^{ac}_{bd}\cdot P[R_i]^{cd}_{ab}}{P[R_i]^{ab}_{cd} P[R_i]^{cd}_{ab}} = \frac{P[R_j]^{ac}_{bd}\cdot P[R_i]^{cd}_{ab}}{\dim[R_i]}. \tag{C11}$$

Apart from the complex, but Hermitian structure $iY_s = P_s[10] - P_s[\overline{10}]$, explicitly

$$i(Y_s)^{ab}_{cd} = \frac{i}{2}(f_{cak}d_{kdb} + d_{cak}f_{kdb}), \tag{C12}$$

which already appeared in the decuplet projectors, the full set of color-singlet four-gluon states includes two more complex, but Hermitian, tensor structures

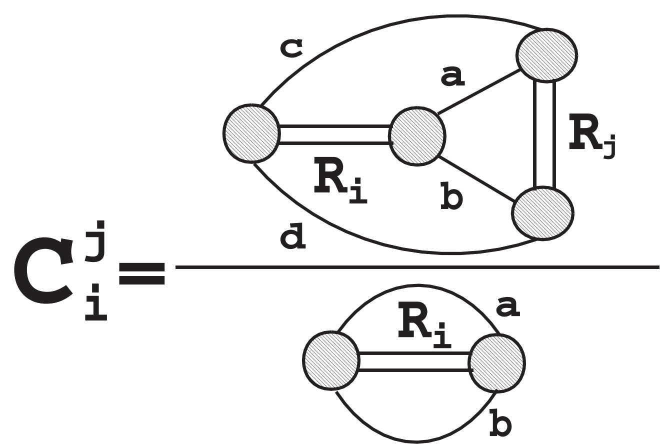

FIG. 7. The matrix element C_i^j of the crossing matrix.

$$
\begin{aligned}
i(Z_s^{(+)})^{ab}_{cd} &= \frac{i}{2}(f_{bak}d_{kcd} + d_{bak}f_{kcd}),\\
i(Z_s^{(-)})^{ab}_{cd} &= \frac{i}{2}(f_{bak}d_{kcd} - d_{bak}f_{kcd}).
\end{aligned}
\tag{C13}
$$

These new tensors $iZ_s^{(\pm)}$ correspond to mixed $|8_A 8_S\rangle$ states. We explicitly introduce the normalized states

$$
\begin{aligned}
|(8_A 8_S)^+\rangle_s &= \sqrt{\frac{2}{(N_c^2-4)(N_c^2-1)}}\, i(Z_s^{(+)})^{ab}_{cd} \\
&\quad \times |g^a(\boldsymbol{b}_1) \otimes g^b(\boldsymbol{b}_2) \otimes g^c(\boldsymbol{b}'_1) \otimes g^d(\boldsymbol{b}'_2)\rangle,\\
|(8_A 8_S)^-\rangle_s &= \sqrt{\frac{2}{(N_c^2-4)(N_c^2-1)}}\, i(Z_s^{(-)})^{ab}_{cd} \\
&\quad \times |g^a(\boldsymbol{b}_1) \otimes g^b(\boldsymbol{b}_2) \otimes g^c(\boldsymbol{b}'_1) \otimes g^d(\boldsymbol{b}'_2)\rangle.
\end{aligned}
\tag{C14}
$$

As mentioned in the main text, these states decouple in the dipole cross section operator (like iY) from the states $|R\bar{R}\rangle_s$ relevant to our problem. It is straightforward to establish their crossing properties, namely,

$$
iY_t = iZ_s^{(-)}, \qquad iZ_t^{(-)} = iY_s, \qquad iZ_t^{(+)} = -iZ_s^{(+)}.
\tag{C15}
$$

Using the projectors derived in Appendix B we then obtain for the crossing matrix, including the complex tensors (C13), the result shown in Eq. (C16), and from there also the basis of eigenstates $|R\bar{R}\rangle_t$ displayed in Eq. (C17). An $SU(3)$ counterpart of the crossing matrix (C16) can be found, e.g. in [39]. Apparently, our crossing matrix could be used for an alternative derivation of the four-gluon dipole cross section matrix. As still another application we notice that, as far as the color algebra is concerned, our calculation of the dipole cross section matrix for the color-singlet four-parton state $ab\bar{c}\,\bar{d}$ is identical to the calculation of the matrix of soft-gluon anomalous dimensions for the scattering process $ab \to cd$ [40]. Here we only want to emphasize that the total number of independent color-singlet states $ab\bar{c}\,\bar{d}$, and the total number of independent amplitudes in $ab \to cd$ scattering thereof, in the s and t channels is the same and the crossing matrix is always a square one.

$$
\begin{pmatrix} P_t[1] \\ P_t[8_A] \\ P_t[8_S] \\ P_t[10] \\ P_t[\overline{10}] \\ P_t[27] \\ P_t[R_7] \\ iZ_t^{(-)} \\ iZ_t^{(+)} \end{pmatrix}
=
\begin{pmatrix}
\frac{1}{N_c^2-1} & \frac{1}{N_c^2-1} & \frac{1}{N_c^2-1} & \frac{1}{N_c^2-1} & \frac{1}{N_c^2-1} & \frac{1}{N_c^2-1} & \frac{1}{N_c^2-1} & 0 & 0 \\
1 & \frac{1}{2} & \frac{1}{2} & 0 & 0 & -\frac{1}{N_c} & \frac{1}{N_c} & 0 & 0 \\
1 & \frac{1}{2} & \frac{1}{2}\frac{N_c^2-12}{N_c^2-4} & -\frac{2}{N_c^2-4} & -\frac{2}{N_c^2-4} & \frac{1}{N_c+2} & -\frac{1}{N_c-2} & 0 & 0 \\
\frac{N_c^2-4}{4} & 0 & -\frac{1}{2} & \frac{1}{4} & \frac{1}{4} & -\frac{1}{4}\frac{N_c-2}{N_c} & -\frac{1}{4}\frac{N_c+2}{N_c} & \frac{1}{2} & 0 \\
\frac{N_c^2-4}{4} & 0 & -\frac{1}{2} & \frac{1}{4} & \frac{1}{4} & -\frac{1}{4}\frac{N_c-2}{N_c} & -\frac{1}{4}\frac{N_c+2}{N_c} & -\frac{1}{2} & 0 \\
\frac{N_c^2(N_c+3)}{4(N_c+1)} & -\frac{N_c}{4}\frac{N_c+3}{N_c+1} & \frac{N_c^2}{4(N_c+2)}\frac{N_c+3}{N_c+1} & -\frac{N_c}{4(N_c+2)}\frac{N_c+3}{N_c+1} & -\frac{N_c}{4(N_c+2)}\frac{N_c+3}{N_c+1} & \frac{N_c^2+N_c+2}{4(N_c+1)(N_c+2)} & \frac{1}{4}\frac{N_c+3}{N_c+1} & 0 & 0 \\
\frac{N_c^2(N_c-3)}{4(N_c-1)} & \frac{N_c}{4}\frac{N_c-3}{N_c-1} & -\frac{N_c^2}{4(N_c-2)}\frac{N_c-3}{N_c-1} & -\frac{N_c}{4(N_c-2)}\frac{N_c-3}{N_c-1} & -\frac{N_c}{4(N_c-2)}\frac{N_c-3}{N_c-1} & \frac{1}{4}\frac{N_c-3}{N_c-1} & \frac{N_c^2-N_c+2}{4(N_c-1)(N_c-2)} & 0 & 0 \\
0 & 0 & 0 & 1 & -1 & 0 & 0 & 0 & 0 \\
0 & 0 & 0 & 0 & 0 & 0 & 0 & 0 & -1
\end{pmatrix}
\times
\begin{pmatrix} P_s[1] \\ P_s[8_A] \\ P_s[8_S] \\ P_s[10] \\ P_s[\overline{10}] \\ P_s[27] \\ P_s[R_7] \\ iZ_s^{(-)} \\ iZ_s^{(+)} \end{pmatrix},
\tag{C16}
$$

$$
\begin{pmatrix} |11\rangle_t \\ |8_A8_A\rangle_t \\ |8_S8_S\rangle_t \\ |10\overline{10}\rangle_t \\ |\overline{10}10\rangle_t \\ |2727\rangle_t \\ |R_7R_7\rangle_t \\ |(8_A8_S)^{(-)}\rangle_t \\ |(8_A8_S)^{(+)}\rangle_t \end{pmatrix} = \begin{pmatrix}
\frac{1}{N_c^2-1} & \frac{1}{\sqrt{N_c^2-1}} & \frac{1}{\sqrt{N_c^2-1}} & \frac{1}{2}\sqrt{\frac{N_c^2-4}{N_c^2-1}} & \frac{1}{2}\sqrt{\frac{N_c^2-4}{N_c^2-1}} & \frac{N_c}{2(N_c+1)}\sqrt{\frac{N_c+3}{N_c-1}} & \frac{N_c}{2(N_c-1)}\sqrt{\frac{N_c-3}{N_c+1}} & 0 & 0 \\
\frac{1}{N_c^2-1} & \frac{1}{2} & \frac{1}{2} & 0 & 0 & -\frac{1}{2}\sqrt{\frac{N_c+3}{N_c+1}} & \frac{1}{2}\sqrt{\frac{N_c-3}{N_c-1}} & 0 & 0 \\
\frac{1}{N_c^2-1} & \frac{1}{2} & \frac{1}{2}\frac{N_c^2-12}{N_c^2-4} & -\frac{1}{\sqrt{N_c^2-4}} & -\frac{1}{\sqrt{N_c^2-4}} & \frac{N_c}{2(N_c+2)}\sqrt{\frac{N_c+3}{N_c+1}} & -\frac{N_c}{2(N_c-2)}\sqrt{\frac{N_c-3}{N_c-1}} & 0 & 0 \\
\frac{1}{2}\sqrt{\frac{N_c^2-4}{N_c^2-1}} & 0 & -\frac{1}{\sqrt{N_c^2-4}} & \frac{1}{4} & \frac{1}{4} & -\frac{1}{4}\sqrt{\frac{N_c-2}{N_c+2}}\sqrt{\frac{N_c+3}{N_c+1}} & -\frac{1}{4}\sqrt{\frac{N_c+2}{N_c-2}}\sqrt{\frac{N_c-3}{N_c-1}} & \frac{1}{\sqrt{2}} & 0 \\
\frac{1}{2}\sqrt{\frac{N_c^2-4}{N_c^2-1}} & 0 & -\frac{1}{\sqrt{N_c^2-4}} & \frac{1}{4} & \frac{1}{4} & -\frac{1}{4}\sqrt{\frac{N_c-2}{N_c+2}}\sqrt{\frac{N_c+3}{N_c+1}} & -\frac{1}{4}\sqrt{\frac{N_c+2}{N_c-2}}\sqrt{\frac{N_c-3}{N_c-1}} & -\frac{1}{\sqrt{2}} & 0 \\
\frac{N_c}{2(N_c+1)}\sqrt{\frac{N_c+3}{N_c-1}} & -\frac{1}{2}\sqrt{\frac{N_c+3}{N_c+1}} & \frac{N_c}{2(N_c+2)}\sqrt{\frac{N_c+3}{N_c+1}} & -\frac{1}{4}\sqrt{\frac{N_c-2}{N_c+2}}\sqrt{\frac{N_c+3}{N_c+1}} & -\frac{1}{4}\sqrt{\frac{N_c-2}{N_c+2}}\sqrt{\frac{N_c+3}{N_c+1}} & \frac{N_c^2+N_c+2}{2(N_c+1)(N_c+2)} & \frac{1}{4}\sqrt{\frac{N_c^2-9}{N_c^2-1}} & 0 & 0 \\
\frac{N_c}{2(N_c-1)}\sqrt{\frac{N_c-3}{N_c+1}} & \frac{1}{2}\sqrt{\frac{N_c-3}{N_c-1}} & -\frac{N_c}{2(N_c-2)}\sqrt{\frac{N_c-3}{N_c-1}} & -\frac{1}{4}\sqrt{\frac{N_c+2}{N_c-2}}\sqrt{\frac{N_c-3}{N_c-1}} & -\frac{1}{4}\sqrt{\frac{N_c+2}{N_c-2}}\sqrt{\frac{N_c-3}{N_c-1}} & \frac{1}{4}\sqrt{\frac{N_c^2-9}{N_c^2-1}} & \frac{N_c^2-N_c+2}{2(N_c-1)(N_c-2)} & 0 & 0 \\
0 & 0 & 0 & \frac{1}{\sqrt{2}} & -\frac{1}{\sqrt{2}} & 0 & 0 & 0 & 0 \\
0 & 0 & 0 & 0 & 0 & 0 & 0 & 0 & -1
\end{pmatrix}
\times \begin{pmatrix} |11\rangle_s \\ |8_A8_A\rangle_s \\ |8_S8_S\rangle_s \\ |10\overline{10}\rangle_s \\ |\overline{10}10\rangle_s \\ |2727\rangle_s \\ |R_7R_7\rangle_s \\ |(8_A8_S)^{(-)}\rangle_s \\ |(8_A8_S)^{(+)}\rangle_s \end{pmatrix} \tag{C17}
$$

APPENDIX D: THE MENAGERIE OF NUCLEAR COLLECTIVE UNINTEGRATED GLUE

A pertinent quantity which emerges in the description of hard processes in a nuclear environment is the collective nuclear unintegrated glue per unit area in the impact parameter space. It is not a single function which can be defined for the whole nucleus, for all hard processes of practical interest the description of the initial and final interactions inevitably calls upon a collective glue for different slices of the nucleus. Furthermore, such a collective glue must be regarded as a density matrix in the space of color representation, i.e., it changes from one reaction to another depending on color properties of the relevant pQCD subprocess [2,4]. One can trace the origin of these variations to the color-representation dependence of the color-dipole cross sections emerging in the description of these reactions.

In the treatment of the nuclear structure function $F_{2A}(x, Q^2)$ and of the quark-antiquark dijets in DIS off nuclei it is advisable to use the collective glue $\phi(\boldsymbol{b}, x, \boldsymbol{\kappa})$ defined in terms of the amplitude of coherent diffractive quark-antiquark dijet production [2,8,41,42]

$$1 - \exp\left[-\frac{1}{2}\sigma_{q\bar{q}}(x, \boldsymbol{r})T(\boldsymbol{b})\right] \equiv \int d^2\boldsymbol{\kappa}\phi(\boldsymbol{b}, x, \boldsymbol{\kappa}) \times [1 - \exp(i\boldsymbol{\kappa}\boldsymbol{r})]. \tag{D1}$$

Here [20,23]

$$\sigma_{q\bar{q}}(x, \boldsymbol{r}) = \int d^2\boldsymbol{\kappa} f(x, \boldsymbol{\kappa})[1 - \exp(i\boldsymbol{\kappa}\boldsymbol{r})], \tag{D2}$$

where

$$f(x, \boldsymbol{\kappa}) = \frac{4\pi\alpha_S(r)}{N_c} \cdot \frac{1}{\kappa^4} \cdot \mathcal{F}(x, \kappa^2), \tag{D3}$$

and

$$\mathcal{F}(x, \kappa^2) = \frac{\partial G(x, \kappa^2)}{\partial \log\kappa^2} \tag{D4}$$

is the unintegrated gluon density in the target nucleon.

The so-defined collective nuclear glue admits a nice probabilistic expansion

$$\phi(\boldsymbol{b}, x, \boldsymbol{\kappa}) = \sum_{j=1} w_{q\bar{q},j}(\nu_A(\boldsymbol{b}))\frac{f^{(j)}(\boldsymbol{\kappa})}{\sigma^j_{q\bar{q},0}}. \tag{D5}$$

Here

$$w_{q\bar{q},j}(\nu_A(\boldsymbol{b})) = \frac{1}{j!}\left[\frac{1}{2}\nu_A(\boldsymbol{b})\right]^j \exp\left[-\frac{1}{2}\nu_A(\boldsymbol{b})\right] \quad \text{(D6)}$$

is a probability to find j spatially overlapping nucleons in the Lorentz-contracted ultrarelativistic nucleus, where

$$\nu_A(\boldsymbol{b}) = \tfrac{1}{2}\sigma_{q\bar{q},0}T(\boldsymbol{b}), \quad \text{(D7)}$$

is the thickness of the nucleus in terms of the number of absorption lengths for large dipoles, and we introduced an auxiliary infrared quantity—a dipole cross section for large quark-antiquark dipoles:

$$\sigma_{0,q\bar{q}} = \int d^2\boldsymbol{\kappa} f(\boldsymbol{\kappa}). \quad \text{(D8)}$$

The properly defined j-fold convolutions,

$$\frac{f^{(j)}(\boldsymbol{\kappa})}{\sigma^j_{q\bar{q},0}} = \int d^2\boldsymbol{\kappa}_1 \frac{f^{(j-1)}(\boldsymbol{\kappa}-\boldsymbol{\kappa}_1)}{\sigma^{j-1}_{q\bar{q},0}} \cdot \frac{f(\boldsymbol{\kappa}_1)}{\sigma_{q\bar{q},0}},$$
$$f^{(0)}(\boldsymbol{\kappa}) = \delta^{(2)}(\boldsymbol{\kappa}), \qquad \int d^2\boldsymbol{\kappa}\frac{f^{(j)}(\boldsymbol{\kappa})}{\sigma^j_{q\bar{q},0}} = 1, \quad \text{(D9)}$$

describe the collective unintegrated glue of j spatially overlapping nucleons in a Lorentz-contracted nucleus. They do not change from one reaction to another, the variations from $\phi(\boldsymbol{b},\boldsymbol{\kappa})$ to $\phi_g(\boldsymbol{b},\boldsymbol{\kappa})$ to $\phi_{gg}(\boldsymbol{b},\boldsymbol{\kappa})$ are fully described by the color-representation dependence of the overlap probabilities:

$$w_{g,j}(\nu_A(\boldsymbol{b})) = w_{q\bar{q},j}\left(\frac{C_A}{2C_F}\nu_A(\boldsymbol{b})\right),$$
$$w_{gg,j}(\nu_A(\boldsymbol{b})) = w_{q\bar{q},j}\left(\frac{C_A}{C_F}\nu_A(\boldsymbol{b})\right). \quad \text{(D10)}$$

[1] E. Leader and E. Predazzi, Cambridge Monogr. Part. Phys., Nucl. Phys., Cosmol. **3**, 1 (1996); **4**, 1 (1996); G. Sterman, *An Introduction to Quantum Field Theory* (Cambridge University Press, Cambridge, England, 1993); R.K. Ellis, W.J. Stirling, and B.R. Webber, Cambridge Monogr. Part. Phys., Nucl. Phys., Cosmol. **8**, 1 (1996).
[2] N.N. Nikolaev, W. Schäfer, B.G. Zakharov, and V.R. Zoller, J. Exp. Theor. Phys. **97**, 441 (2003) [Zh. Eksp. Teor. Fiz. **124**, 491 (2003)].
[3] N.N. Nikolaev, W. Schäfer, B.G. Zakharov, and V.R. Zoller, Phys. At. Nucl. **68**, 661 (2005) [Yad. Fiz. **68**, 692 (2005)].
[4] N.N. Nikolaev and W. Schäfer, Phys. Rev. D **71**, 014023 (2005).
[5] N.N. Nikolaev, W. Schäfer, and B.G. Zakharov, Phys. Rev. Lett. **95**, 221 803 (2005).
[6] N.N. Nikolaev, W. Schäfer, B.G. Zakharov, and V.R. Zoller, Phys. Rev. D **72**, 034033 (2005).
[7] N.N. Nikolaev and B.G. Zakharov, Phys. Lett. B **332**, 177 (1994).
[8] N.N. Nikolaev, W. Schäfer, and G. Schwiete, Phys. Rev. D **63**, 014020 (2001).
[9] E.A. Kuraev, L.N. Lipatov, and V.S. Fadin, Sov. Phys. JETP **45**, 199 (1977) [Zh. Eksp. Teor. Fiz. **72**, 377 (1977)].
[10] S. Kretzer, Acta Phys. Pol. B **36**, 179 (2005).
[11] N.N. Nikolaev, G. Piller, and B.G. Zakharov, J. Exp. Theor. Phys. **81**, 851 (1995) [Zh. Eksp. Teor. Fiz. **108**, 1554 (1995)]; Z. Phys. A **354**, 99 (1996).
[12] B.G. Zakharov, Yad. Fiz. **46**, 148 (1987) [Sov. J. Nucl. Phys. **46**, 92 (1987)].
[13] B.G. Zakharov, JETP Lett. **63**, 952 (1996); JETP Lett. **65**, 615 (1997); Phys. At. Nucl. **61**, 838 (1998) [Yad. Fiz. **61**, 924 (1998)]; R. Baier, D. Schiff, and B.G. Zakharov, Annu. Rev. Nucl. Part. Sci. **50**, 37 (2000).
[14] J. Jalilian-Marian and Y.V. Kovchegov, Phys. Rev. D **70**, 114017 (2004).
[15] R. Baier, A. Kovner, M. Nardi, and U.A. Wiedemann, Phys. Rev. D **72**, 094013 (2005).
[16] J.D. Bjorken, Phys. Rev. D **47**, 101 (1993).
[17] N.N. Nikolaev and V.I. Zakharov, Sov. J. Nucl. Phys. **21**, 227 (1975) [Yad. Fiz. **21**, 434 (1975)]; Phys. Lett. B **55**, 397 (1975).
[18] N.N. Nikolaev and B.G. Zakharov, Z. Phys. C **49**, 607 (1991).
[19] N.N. Nikolaev and B.G. Zakharov, Z. Phys. C **53**, 331 (1992).
[20] N.N. Nikolaev and B.G. Zakharov, J. Exp. Theor. Phys. **78**, 598 (1994); [Zh. Eksp. Teor. Fiz. **105**, 1117 (1994)]; N.N. Nikolaev and B.G. Zakharov, Z. Phys. C **64**, 631 (1994).
[21] R.J. Glauber, in *Lectures in Theoretical Physics*, edited by W.E. Brittin *et al.* (Interscience, New York, 1959), Vol. 1, p. 315.
[22] V.N. Gribov, Sov. Phys. JETP **29**, 483 (1969); [Zh. Eksp. Teor. Fiz. **56**, 892 (1969)].
[23] N.N. Nikolaev and B.G. Zakharov, Phys. Lett. B **332**, 184 (1994).
[24] N.N. Nikolaev, B.G. Zakharov, and V.R. Zoller, JETP Lett. **59**, 6 (1994).

[25] I. I. Balitsky and L. N. Lipatov, Sov. J. Nucl. Phys. **28**, 822 (1978); [Yad. Fiz. **28**, 1597 (1978)].
[26] P. Cvitanović, Group Theory, Webbook version 8.3.7, http://www.nbi.dk/GroupTheory/.
[27] B. Z. Kopeliovich and B. G. Zakharov, Z. Phys. C **43**, 241 (1989).
[28] B. Z. Kopeliovich and B. G. Zakharov, Phys. Lett. B **211**, 221 (1988).
[29] B. Z. Kopeliovich and B. G. Zakharov, Sov. J. Part. Nuclei **22**, 136 (1991) [Fiz. Elem. Chastits At. Yadra **22**, 140, 1991].
[30] E. V. Shuryak, Rev. Mod. Phys. **65**, 1 (1993); E. Meggiolaro, Phys. Lett. B **451**, 414 (1999).
[31] A. B. Kaidalov, Phys. Lett. **116B**, 459 (1982); A. Capella and J. TranThanh Van, Phys. Lett. **114B**, 450 (1982).
[32] A. Casher, H. Neuberger, and S. Nussinov, Phys. Rev. D **20**, 179 (1979).
[33] L. Montanet, G. C. Rossi, and G. Veneziano, Phys. Rep. **63**, 149 (1980).
[34] B. G. Zakharov, *Proceedings of the 33rd Rencontres de Moriond: QCD and High Energy Hadronic Interactions, Les Arcs, France, 1998*, p. 465; hep-ph/9807396.
[35] P. Aurenche and B. G. Zakharov (work in progress).
[36] J. Adams *et al.* (STAR Collaboration), Nucl. Phys. **A757**, 102 (2005).
[37] A. J. MacFarlane, A. Sudbery, and P. H. Weisz, Commun. Math. Phys. **11**, 77 (1968).
[38] J. A. de Azcarraga, A. J. Macfarlane, A. J. Mountain, and J. C. Perez Bueno, Nucl. Phys. **B510**, 657 (1998).
[39] C. Rebbi and R. Slansky, Rev. Mod. Phys. **42**, 68 (1970).
[40] Y. L. Dokshitzer and G. Marchesini, hep-ph/0508130; M. H. Seymour, J. High Energy Phys. 10 (2005) 029.
[41] N. N. Nikolaev, W. Schäfer, and G. Schwiete, JETP Lett. **72**, 405 (2000) [Pis'ma Zh. Eksp. Teor. Fiz. **72**, 583 (2000)].
[42] N. N. Nikolaev, W. Schäfer, B. G. Zakharov, and V. R. Zoller, JETP Lett. **76**, 195 (2002); [Pis'ma Zh. Eksp. Teor. Fiz. **76**, 231 (2002)].